SCRATCH OF POLYMERS - MODELING ABRASIVE WEAR

Wending Gu

Abstract— In this paper, the influence of the indenter geometry on the scratch performance of single-phase polymer and the scratch and wear properties of the reinforced multi-phase polymer by filling the particles were studied. Finite element method is mainly applied in this paper for the analysis of simulation results. Indenters with three different types of geometry were designed for indentation and scratching test of neat epoxy matrix, and it was found that the stress - strain field and residual scratch depth of single - phase polymer surface were significantly affected by the indenter sharpness. Furthermore, in order to in-depth understand the scratch behavior of polymer composites after particle reinforcement, soft rubber and hard silica particles with different concentrations, particle sizes were modeled and filled into the epoxy matrix at different positions underneath the material surface. In the end, the influence of loading conditions and the rubber particle concentration on the friction coefficient and wear mass loss of polymer composites during the wear process was also investigated.

Keywords— • FEM • Polymer composites • Indentation performance • Scratch behaviour • Damage mechanisms • Wear Property • Frictional coefficient

CHAPTER I: INTRODUCTION

1.1 Background

Polymer materials are more susceptible to severe surface damage, especially scratches, than ordinary materials in most industrial applications. The scratch resistance and wear resistance of the polymer determine the degree of damage that it can withstand the sliding indentation of sharp objects on its rough surface.

The scratch and wear properties of polymers have attracted considerable attention over the past decade because of their wide applications in electronics, optics and automotive applications, where long-term aesthetics are important. Unlike ceramics and metals, polymer composites are particularly prone to surface deformation and damage, even at low contact loads. The scratch process here is defined as a mechanical deformation process in which a controlled force or displacement acts on a hard spherical tip, pressing it into a polymer matrix, and moving its on the matrix surface at a specified speed. It should be noted that the thickness of polymer matrix, surface properties, the geometry and material properties of the indenter, as well as the test rate, all have significant effects on the scratch performance of the polymer.

1.2 Research of polymer scratch

The deformation of polymer surface caused by scratch tip is a complex mechanical process. The surface damage patterns of polymer materials can be classified as brittle damage such as cracking and fracture and ductile damage such as shear yield. Studies have shown that the scratches damage patterns are determined by the properties of the material and the amount of load applied. The surface damage patterns of polymer materials can be classified as brittle damage such as cracking and fracture and ductile damage such as shear yield. Studies have shown that the scratches damage patterns are determined by the properties of the material and state and magnitude of stress applied [1,2]. With the development of polymer science and technology, it is easier to understand the complex stress field and nonlinear characteristics of polymers caused by its scratch behavior. At present, the scratch map and finite element modeling are the main methods used for the visual research of polymer scratches. The scratch map method is mainly used to correlate the friction data in the experiment with the surface deformation mechanism of the polymer material, but the scratch map cannot describe the damage mechanism of the polymer surface in detail in all cases and the scratch map method relies on qualitative assessment. It was not until 2003 that the ASTM standard for linear loading scratches test was introduced to more objectively test the scratches deformation of polymers such as fish scales and micro-cracks to evaluate the scratch resistance of polymers [3]. In general, it is not realistic to control a group of material properties during the scratch experiment, but the finite element method can control a single material property variable for more accurate parameterized research. Based on the finite element modeling method, it was found that the formation of scratch grooves on the surface of polymer materials was mainly determined by its compression performance and its surface damage mode was affected by the surface characteristics of the material, thus the guiding principles for the design of anti-scratch polymers were proposed [4-6]. Based on these studies, this project mainly used ABAQUS software for modeling and carried out finite element analysis of the scratch behavior of polymer composite.

1.3 Objective of study

The purpose of this project is to study the indentation, scratch and wear properties of polymer especially multi-phase polymer composites. Since the brittleness, toughness and low tensile properties of single-phase polymers such as pure epoxy limit their application space in various industries, the material properties of polymer composites, preparation techniques and mechanical properties of nano-fillers used to reinforce multi-

phase polymers have been widely studied by scholars. Based on the review of existing literature, it is found that although scholars have carried out amount of experimental studies from various aspects such as the types of polymer composites, dispersion degree of particles, size and concentration of fillers, and some findings were obtained, these results are one-sided and contradictory. Also, the damage mechanism of multi-phase polymer surface is complex and lack of relevant research. Based on these problems, ABAQUS and the Finite Element Method (FEM) were employed in this project to design and simulate the indentation and scratch test of neat epoxy matrix, the scratch test of epoxy microcomposite modified by soft rubber and hard silica particles, and the wear test of epoxy microcomposite modified by soft rubber particles. It is expected that the models established in this project can be applied to any polymer and polymer composites, and simulation results of this project will be able to use to improve the mechanical performance of engineering plastic parts, industrial coatings and military radar stealth coatings for multiple applications.

1.4 Outline

•*Chapter I* introduces the background of scratching of polymers - modeling abrasive wear and sets out clearly the purposes of this project.

•*Chapter II* presents a literature review on the scratch and wear behaviour of polymers

•*Chapter III* describes in detail the three main research designs of the project, and discusses the model configuration parameters, necessary simulation requirements and objectives of each step.

•*Chapter IV* presents the simulation results for each research design and compares the results for in-depth analysis based on current research background from the literature.

•*Chapter V* concludes the findings obtained through finite element modeling analysis in the thesis and provides the recommendations for future studies.

CHAPTER II: LITERATURE REVIEW

2.1 Research background and significance

Polymer materials are usually classified as single-phase and multi-phase polymers. Single-phase polymer is widely used in industrial applications, and the surface of single-phase polymer material is easy to be scratched to affect its performance. Scratch resistance is one of the most important properties of materials. Surface damage characteristics such as linear loading, tillage, microcracks and fish scales are formed by applying linear loading on the polymer surface, and these characteristics are influenced by the polymer surface state and loading value.

To compare with single-phase polymer, the damage caused by scratch of multi-phase polymer is independent of its properties. In multi-phase polymer systems, there is no clear relationship between material properties and scratches - induced damage characteristics. Since multi-phase polymer also can be easily scratched, thus to improve its material surface scratch resistance not only considering the aesthetic of material, but also in order to maintain the integrity of the structure of the polymer surface by adding protection coating. Although multi-phase polymer systems have been widely used in industrial products, there are few numerical simulation studies on scratch damage. Therefore, it is necessary and urgent to study the scratch behaviour and wear performance of multi-phase polymer such as epoxy nanocomposites.

2.2 Development history of nanomaterials

Nanomaterials are regarded as the most valuable and promising materials in the 21st century because of their unique properties [7]. It is not only urgent to perfect the theoretical research basis, but also of great research significance in practical applications. A nanoparticle is a particle with a particle size of 1 to 100nm and its volume or surface effect can be observed [8]. Nanoparticles are usually composed of a small number of atoms or molecules. The special arrangement of the surface and intermediate atoms of nanoparticles results in special surface and volume effects, which obviously affects the physical and chemical properties of nanoparticles. In 1861, Thomas, a British chemist, first conducted research on nanomaterials and coined the term colloidal to represent all suspensions containing nanoparticles of unequal diameter [9]. Half a century later, a method called LB(Langmuir-Blodgett) for preparing nanomaterials was developed. In 1959, renowned physicist Richard Feynman first defined the concept of nanotechnology. Since 1960, chemical reactors, plasmas and electric arcs had been used to make ultrafine particles. In 1962, Japanese scientists theoretically studied the quantum size effect of nanoparticles. In the 1980s, nanomaterials science developed rapidly due to the improvement of observation technology and the progress of mesoscopic physics. The first discovery of carbon nanotubes in 1991 had made it possible to produce today's nanomaterials such as nanoparticles, nanowires, carbon nanotubes and nanofilms [10-12]. The concept of nanocomposites originated in the late 1980s, which is a new type of composites developed rapidly in recent years. Nanocomposites consists of at least one nanoscale material and other materials. At the present, common polymer nanocomposites are based on an organic polymer matrix such as epoxy and filled with nanoparticles as a reinforcing agent. It is different from the polymer system modified by traditional material fillers that nanocomposites are not only the common combination of all phase materials, but also the composite at the nano-scale. The small size of nano-filled particles leads to a large interface between the matrix and the dispersed phase, which makes the interface fuzzy. Therefore, the properties of nano-fillers enable nanocomposites to have numerous excellent properties and wide application prospects.

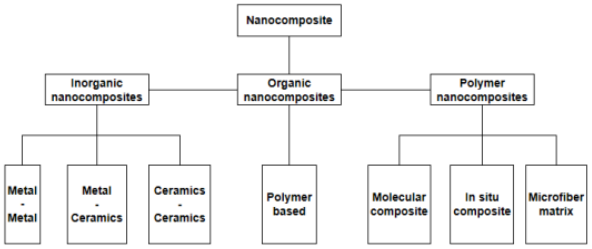

Figure 1 Classification of nanocomposites

2.3 Research status of particle modified polymer nanocomposites

The properties of polymers filled with nano-scale particles are quite different from those filled with traditional particles. Some properties of polymer nanocomposites, such as tensile strength and modulus, can also be obtained by filling with micron particles of a higher volume. Some properties, such as barrier property and transparency, are not available in traditional composite materials. Several research results [13,14] showed that, different from the traditional modified epoxy resin method, the addition of appropriate amount of nanoparticles can not only significantly improve the mechanical properties of the matrix, but also improve the overall thermal properties of the material in some systems [15]. With the development of nanomaterials preparation technology and the commercialization of nanomaterials, the use advantages of nanoparticles are becoming more and more obvious from the perspective of performance stability and cost. Therefore, the application of nanoparticle modified epoxy system has attracted more and more attention. According to the morphology of dispersed phase, polymer nanocomposites can be divided into three categories: dispersed phase is nanoscale in three dimensions (such as spherical particles), dispersed phase is nanoscale in two dimensions (such as clay lamellae), and dispersed phase is nanoscale only in one dimension (such as carbon nanotubes and whiskers). According to the material category of dispersed phase, polymer nanocomposites can be divided into polymer, inorganic particles, polymer/metal and other nanocomposites. According to the final use of nanocomposites, nanocomposites can be divided into structural composites and functional composites. In recent years, nanocomposites have obtained superior properties due to the modification of nanoparticles. For example, the addition of inorganic nanoparticles can toughen and strengthen the epoxy resin system at the same time [16, 17]. At the same time, the addition of functional nanomaterials also enables the polymer matrix to be flame retardant and heat resistant [18].

According to the different types of nanoparticles filled, epoxy based nanocomposites can be divided into the following types:

***(1) Nanoclay modified epoxy* nanocomposites**

Nano clay is a commonly used epoxy resin modified filler. Nano clay is a two-dimensional layered reinforced phase, and the distance between the sheets is generally up to the nanometer level. When the polymer is embedded in the layers, "embedded nanocomposite" can be formed, while when the sheets are dispersed in the polymer, "layered nano-composite" can be formed. The preparation technology of nano-clay is divided into intercalation method and exfoliation method. Wang et al. [19] prepared a nano-clay filled epoxy resin composite with high peeling and good dispersion. At the same time, the experimental results showed that the modified clay nanocomposites, and toughness was increased significantly, the modulus and strength slightly reduced. Recently, Sun et al. [20] prepared highly dispersed carbon nanotubes and layered zirconium phosphate mixed modified epoxy resin, it was found that the tensile modulus, strength and elongation at break of epoxy resin were significantly improved.

(2) Carbon nanotubes modified epoxy nanocomposites

Carbon nanotubes were first discovered in 1991. As one-dimensional nanomaterials, they are often used as reinforcing phases of polymer materials. The diameter of carbon nanotubes is only one of several thousand times that of carbon fibers, which has better mechanical properties, high strength and fracture ductility than carbon fibers. Studies on electrical properties show that adding carbon nanotubes can significantly improve the electrical conductivity of the material. Compared with the addition of carbon black to improve the electrical conductivity of the material, carbon nanotubes can significantly reduce the volume content of the required filler. At the same time, the carbon nanotubes have good flexibility and short length, which can be added into the polymer without fracture and maintain the ratio of height to fineness. Studies have shown that the conductivity of plastics with 2%-3% MWNT can be significantly increased from 10-12s/m to 102s/m.

Whether carbon nanotubes (CNTS) can be highly dispersed in the matrix and the interface of CNTS/matrix are the key factors for the preparation of high-performance CNT modified epoxy matrix composites [21]. Song and Youn [22] found that well-dispersed multi-wall carbon nanotubes had a more obvious improvement in the tensile and conductive properties of the materials. The study on Thostenson[23] 's influence on the preparation process showed that mechanical agitation with high shear action could disperse carbon nanotubes better, and the experimental performance results showed that carbon nanotubes could significantly provide the fracture performance of epoxy matrix. At present, there are still some thorny problems to be solved in the research of carbon nanotubes modified epoxy nanocomposites. How to control the dispersion uniformity and orientation of carbon nanotubes as well as the interaction and failure mechanism of carbon nanotubes/matrix interface need to be further improved.

(3) Rigid inorganic nanoparticles modified epoxy nanocomposites

Based on the previous idea of modified micron rubber elastomer, the method of modified epoxy resin by nano flexible particles was developed gradually. The difference was found that that nanometer flexible particles were better than traditional

rubber elastomers for toughening. Although nanometer rubber particles have basically the same effect as traditional rubber when the content of the two is roughly the same, the former can significantly reduce the loss of material modulus [24-26]. In recent years, with the development of the manufacturing technology and surface treatment technology of inorganic particles, the toughening method of inorganic rigid nanoparticles has become more and more mature, which overturns the traditional modification method of rubber elastomer matrix. Three-dimensional rigid nanoparticles can improve the strength of brittle polymers while toughening them. The remarkable effect of rigid nanoparticles on the toughening and strengthening of polymer matrix has attracted more and more attention from scholars in the field of composites mechanics. In recent years, many scholars have studied the rigid particle modified polymer system, and the results show that the mechanical properties of nano-rigid particle modified polymer system are affected by many factors, such as particle dispersion degree, particle content, particle/matrix interface and particle size.

The elastic modulus of rigid particles is much larger than that of polymer matrix, thus the stiffness of the modified polymer system can be improved obviously even if the addition of rigid nanoparticles brings some agglomeration [49], and when the size of particle agglomeration is too large, it will have a negative impact on the stiffness of materials [50]. The agglomeration of nanoparticles can also significantly reduce the strength and elongation at break of modified epoxy systems [50]. The experimental results also show that the fracture and impact toughness of the modified system can be significantly improved when there is a small amount of agglomeration in the matrix [51]. A small amount of nanoparticle aggregates can lead to partial crack toughening mechanism, so that both the extended crack and the rough fracture surface can consume more energy and improve the fracture toughness of materials [52]. As a result, the dispersion degree and agglomeration phenomenon of nanoparticles can affect the mechanical properties of epoxy resin matrix, and the related mechanism is complex.

For the modified system with good dispersion of nanoparticles in the matrix, the increasing of particle content can gradually improve the overall stiffness of the nanocomposite, but the influence on the overall strength of the modified system is different. It is generally believed that the strength of the modified system is proportional to the content of the nano fillers [56]. Mahrholz et al. [57] showed that the increase of nanoparticle silica content had a significant influence on the increase of bending strength of epoxy resin after modification. G. Ragosta et al. [55] also showed that under the condition of good nanoparticle dispersion, the enhancement effect of nano silica on epoxy resin system was closely related to its content increase. Some results [58] show that the content of rigid nanoparticles has no obvious effect on the strength of the matrix. Zhao et al. [53] found that using the different volume fraction of alumina particles to modify the epoxy resin matrix, the strength of the nanocomposites are almost constant. At the same time, some experimental results [54] show that with the increase of nano silicon dioxide content, the strength of the nanocomposites are stable within a certain range at first and then increases. When the particle concentration reaches a certain value, there is a downward trend in intensity. In summary, for nanocomposite systems with well-dispersed particles, the rigidity and toughness of epoxy resin increase with the increase of the content of rigid nanoparticles.

The interface of inorganic nanoparticles or matrix is also an important factor affecting the overall mechanical properties of nanocomposites. Studies [53] have shown that for epoxy resin systems with good dispersion, the interfacial properties of particles and matrix have little influence on the overall stiffness, but the effect on epoxy resin system with poor dispersion is more obvious. The surface modification of nanoparticles can directly affect the interaction of particles or matrix, which is beneficial to the dispersion of nanoparticles in the matrix and improve the mechanical properties of epoxy resin, such as elastic modulus, strength and toughness. The interfacial properties between nanoparticles and matrix directly affect the stress transfer between them, thus affecting the strength of nanocomposites. Therefore, the strength of materials is closely related to the interfacial properties of particles/matrix. Guo[59] et al. found in their study that the addition of 3% nano-scale Al203 without surface modification reduced the strength of the nanocomposite by up to 24%, while the overall strength of the material was significantly improved after surface treatment of the nanoparticles. Therefore, the interfacial properties affect the toughening mechanism of the nanocomposites and the decohesion of the matrix plastic deformation particles and the growth of plastic holes may be the main factors to restrain the crack propagation.

2.4 Scratch behaviour of particle modified polymer nanocomposites

From the 1950s to the beginning of this century, the research on scratch properties of materials only focused on metal and ceramic materials. With the wide application of plastic engineering parts and polymer composite coatings in the field of industrial production, people started to pay more attention to the scratch behavior of polymer materials [39-41]. Since the establishment of ISO(DIS 19252) and ASTM(D7027-05) [42] which are about linearly increasing load test standards, engineers have been able to use this standard to study scratch visibility, depth, and friction coefficient on the surface of polymer materials to evaluate scratch performance of polymers more systematically. In addition, nanotechnology and micro-particle preparation technology are widely used to enhance the mechanical and chemical properties of polymer composites. According to the finite element study on the scratch behavior of polymer nanocomposite by Wang et al. [43], it could be found that during the scratch process, the load was transferred from the epoxy matrix to silica nanoparticles gradually, thus to enhance the scratch resistance of epoxy nanocomposite. Based on the research of Moghbelli et al.[44], it could be found that the filling of hard fillers were able to improve the modulus and strength of multi-phase polymer materials. Also, the toughness of polymers could be increased by filling soft fillers.

However, the scratch performance of multi-phase polymer could not be improved by adding neither soft nor rigid fillers. This phenomenon may be due to the mechanical properties of multi-phase polymers affected by particle size, load and interface adhesion. Moreover, Kurkcu et al. [45] studied the friction and wear properties of SAN - and epoxy-based composites and found that adding 100 μm hard fillers could change the scratch pattern of the polymer composites from ductile to brittle, thus improving the scratch resistance of the materials. On the contrary, it was found that the filling of soft fillers (Fortegra 100) worsened the scratch property of polymer composites. Furthermore, Hossain et al.[46] studied the acrylonitrile styrene acrylate particle modified nano-composite and found that the rubber particles with a filling size of 1 μm can better improve the scratch resistance of polymer nanocomposites. This is due to that only 1 μm of rubber particles can cover the surface of the material after the material has been annealed at high temperature to reduce the possibility of cracking. Ng et al.[47] studied the scratch properties of titanium dioxide nano- and micro-particles modified epoxy composite materials and then the results showed that 32 nm titanium carbide modified epoxy composites have the best scratch resistance. Finally, the research results of Wang and Lim [48] also showed that the scratch visibility of the polymer nanocomposite reinforced by tungsten carbide particles was lower than that of neat polymer materials.

2.5 Wear property of polymer nanocomposites

With the deepening of the research on materials science, the technology of micro-particle modified polymers has been paid more attention and developed rapidly. Based on the current research of Wang et al. [27-32], it was found that the friction coefficient and wear rate of PEEK nanocomposites modified by silicon nitride nanoparticles were much lower than PEEK matrix itself. When the volume fraction of silicon nitride nanoparticles is 7.5%, the wear rate was the lowest and PEEK material wear performance was not constrained by its mechanical properties. X-ray photoelectron spectroscopy (XPS) was used to observe silicon nitride nanoparticles, and it was known that they were oxidized to partial silica and formed a uniform layer of transfer film on their dual surface. Wang et al.[27-33] also studied the friction and wear properties of silica nanoparticles modified PEEK composite and found that the results were similar to those of silicon nitride particle modification. In the subsequent study on the wear behavior of PEEK composite modified by nano-scale and micro-scale silicon carbide particles with different particle sizes and silicon carbide whisker, the wear mechanism was analyzed and the conclusion was reached that the filling of silicon carbide particles reduced the friction coefficient of PEEK composite. The results showed that the addition of 10wt% silicon carbide nanoparticles could effectively reduce the wear rate of PEEK composite and the filling of the same content of silicon carbide microparticles could improve the wear resistance of the material, but modified with silicon carbide whisker could not reduce the wear rate of the material. The surface and dual surface of the PEEK composite modified by silicon carbide micro-whisker appeared continuously distributed rough furrows, and a relatively thick layer of transfer film was formed, thus abrasive wear and furrows were the main wear modes of PEEK composite modified by silicon carbide micro-whisker. In contrast, the silicon carbide nanopatricles modified PEEK composite had a smooth and flat surface without marks made by adhesion and furrow. The dual surface of the silicon carbide nanopatricles modified PEEK composite was also smooth and a layer transfer film was formed with a tight adhesion to the substrate. These results indicated that the filling of silicon carbide nanoparticles could effectively improve the abrasion resistance and wear mode of PEEK composite mainly consists of slight adhesion wear.

In order to study the mechanism of nanoparticles improving the friction and wear properties of polymers, Christian et al. [34] measured the force between the transfer membrane of aluminium oxide nanoparticles modified PPS composites and the dual surface. The results showed that when aluminium oxide nanoparticles with 2% concentration were filled into PPS materials with a roughness Ra of 0.06 and 1 micron, the wear rate was reduced by increasing the force between the transfer film and the dual surface. However, when the roughness of the dual surface of PPS material was 0.027 micron, the force between the transfer film and the dual surface was too small, which resulted in the incomplete formation of the transfer film and the increase of wear rate. Christian et al. also found that there was no specific relationship between the concentration of filled aluminium oxide nanoparticles and the wear rate, and only filling the aluminium oxide nanoparticles with a concentration of 2% could minimize the wear rate of the material. Moreover, it had been shown that the best wear-resisting performance of PPS composites needed to be filled with a minimum concentration of 25-30vol% aluminium oxide microparticles [35-38]. Filling with aluminium oxide nanoparticles reduced the wear rate of PPS composites by 1.4 times and only increases the friction coefficient slightly. In comparison, the wear rate of copper oxide micro-particle modified PEEK system decreased by 14.2 times [35], the wear rate of copper sulfide micro-particle enhanced PEEK composite decreased by 11.4 times [35], and the wear rate of silver sulfide microparticle modified PPS composite decreased by 4.5 times [28-29]. This difference could be attributed to the high inertia of aluminium oxide nanoparticles and the failure of chemical reaction with the material dual surface. However, copper oxide, copper sulfide and silver sulfide micro-particles could react with the material dual surface, resulting in a significant reduction in wear rate. Consistent with the previous findings of Wang et al. [30], the mechanical properties of polymer materials could not affect their wear rate.

2.6 Review

With the development of modern industries, the demand for material properties in many fields is also increasing, and modern materials are moving towards the direction of composite and multifunctional. Polymers have gradually replaced traditional materials such as metal and ceramic to become widely used materials, thus the research on scratch wear properties of

polymers, especially polymer nanocomposites, cannot be ignored. Since the brittleness, toughness, low strength and low tensile properties of single-phase polymers make them unsuitable for most applications, a number of studies have been conducted on multi-phase polymers by numerous scholars but the results are mixed. For example, some research results indicated that the concentration of rigid nanoparticles could not affect the strength of polymer matrix, while the research data of G. Ragosta et al.[55] proved that the content of rigid silica was closely related to the strengthening effect of epoxy nanocomposite materials. From the information collected so far in this paper, although scholars have conducted relevant experiments and studies from the perspectives of material types and properties, size and concentration of nano-fillers, preparation of nanocomposite materials, and dispersion mode of nanoparticles, environmental factors, interface factors of particle or matrix and theoretical differences of these studies make these studies one-sidedness and still have numerous various deficiencies.

CHAPTER III: RESEARCH DESIGN AND MODELING

3.1 Design One: Indentation and scratch test of single-phase polymer

3.1.1 Design requirements and aims

Firstly, this simulation design was about the indentation and scratch tests on the surface of a neat epoxy matrix with different geometric indenters. Three types of indenters were designed as spherical indenter, blunt conical indenter and.sharp conical indenter. Also, the length, thickness and width of the neat epoxy model were set as 5mm, 1mm and 1mm respectively. The bottom and end nodes of the model were constrained in three directions and nodes on a plane of symmetry were constrained in the normal direction. Since epoxy was brittle and strong polymer, the three kinds of indenters designed in this model were made of rigid materials and the diameter of indenters was 1mm. Also, this scratch test was carried out based on linear increasing load ASTM standard. Indentation, scratching and rebounding were the three main steps during this finite element simulation process. During the simulation process, the coulomb friction model was adopted and the friction coefficient between the indenter tip and the surface of the epoxy matrix was set as 0.3.

Furthermore, the normal load applied on the indenter tip was 20N and the distance of scratch was 3mm. The analysis of explicit dynamic stress was applied in this finite element modeling simulation due to the dynamic process of scratching. In order to reduce the computational time and complexity of the simulation, heat transfer and velocity variations were not taken into account and the scratching speed was set at a constant 6 m/s. The three dimensional linear brick element was applied in this simulation model. In the end, since the spherical indenter was designed to be 1mm in diameter and 1.5mm in height, for controlling variable analysis, the diameter and length of the blunt and sharp conical indenter were designed the same as that of the spherical indenter. Therefore, the influence of indenter sharpness on the scratch depth and the surface stress and strain of pure epoxy matrix could be studied.

3.1.2 Indenter Geometry

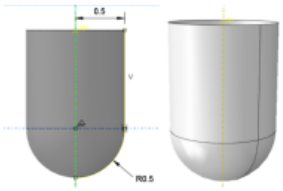

Figure 2 Spherical indenter geometry and model

The typical rigid spherical indenter is shown in Figure 2 above. Since it does not have a sharp tip, it is assumed that the scratches grooves caused by scratching the polymer surface with the spherical indenter of this design are the shallowest and the damage pattern of the material surface is relatively simple.

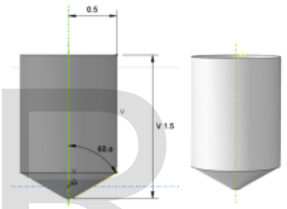

Figure 3 Blunt conical indenter geometry and model

Compared with the spherical indenter, the tip of the blunt conical indenter is made of a blunt circle and the angle of the tip is 120 degrees. Therefore, it is assumed that scratching the surface of epoxy matrix with a blunt conical indenter will lead to deeper scratch depth and a relatively complex damage mechanism.

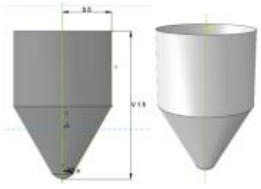

Figure 4 Sharp conical indenter geometry and model

Among the three types of indenter, the tip of the acute conical indenter is the sharpest. Scratching the epoxy matrix with a sharp conical indenter may result in the deepest scratch depth and more irreversible plastic deformation on the surface of a pure epoxy matrix than a spherical indenter or a blunt conical indenter.

Table 1 Indenter geometry parameters

Shapes	Diameters(mm)	Heights (mm)	Tip Angles
Spherical	1	1.5	-
Blunt conical	1	1.5	120°
Sharp conical	1	1.5	60°

Subsequent sets of simulated indentation and scratch tests will verify these assumptions. In addition, the influence of three kinds of rigid indenters with different geometric shapes on the stress and strain of neat epoxy matrix and the simulation results will be obtained. Details of the indenter geometry are recorded in the above table 1. Variables such as the indenter diameter and length are controlled since only the impact of the indenter sharpness on the scratches behavior of the polymer is considered.

3.1.3 Material Properties

Table 2 Material properties of epoxy matrix

Material Properties	Density (tonne/mm^3)	Young's Modulus (GPa)
Epoxy	2.25E-006	3

Material Properties	Poisson's Ratio	Yield Stress (MPa)	Strain Hardening Slope(MPa)
Epoxy	0.32	80	100

In order to obtain the best simulation results, according to the established simulation requirements, the material performance parameters of density, elasticity and plasticity are selected and set as shown in the table 2. The figure and table above describe in detail the material properties of a neat epoxy matrix.

Compared with other polymer materials, pure epoxy is a brittle and strong polymer, and its young's modulus of only 3 GPa also indicates its weak deformation resistance. The yield stress refers to the normal stress magnitude of the material when yielding occurs. During the process of the epoxy matrix being stretched or compressed by external forces, when the stress reaches the critical value, it slightly increases while the strain increases sharply, indicating the epoxy matrix yielding occurs. However, the critical stress magnitude cannot be directly obtained and it is determined by different material properties. The yield stress of epoxy matrix set in this part is 80 MPa, which is much lower than that of cermet and metal materials.

Also, the poisson's ratio for neat epoxy was set as 0.32 in this simulation. Poisson's ratio is the absolute value of the ratio between the transverse strain and the corresponding longitudinal strain caused by the uniformly distributed longitudinal stress on the epoxy matrix.

Furthermore, the strain hardening slope of epoxy matrix is set as 100 MPa. The strain hardening slope, also known as strain hardening modulus, is usually used to describe the phenomenon that the lattice of a material is distorted after plastic deformation, thus improving the anti-deformation performance of the polymer materials.

3.1.4 Simulation Models

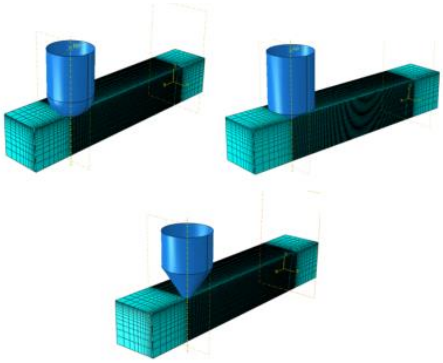

Figure 5 Basic models of indentation and scratch tests on epoxy matrix

The first step to simulate indentation and scratch test is to construct the basic model of epoxy matrix and three kinds of indentation indenters. As shown in the Figure 5 above, the epoxy matrix is meshed and the meshing density in the middle region of the matrix is greater than that at both ends. According to the established boundary conditions, both ends of the pure epoxy matrix are fixed and the scratch process is mainly carried out in the middle region of the matrix. Also, the epoxy matrix is cuboid with size of 1x1x5 mm. The initial position of all three geometry indenters is set to be perpendicular to and in perfect contact with the surface. Moreover, In order to improve the visibility of the stress-strain profile and scratch groove simulated in the next step, the indentation and scratch process of the indenter are carried out along the upper surface edge of the cuboid substrate, thus to better analyze and compare the three-dimensional distribution of von Mises stress, plastic strain and maximum principal stress.

3.2 Design Two: Scratch test of polymer microcomposites

3.2.1 Design requirements and aims

It is well understood the preparation process of nano-scale particle modified materials are complex and expensive. As a result, the the second design mainly focused on the scratch tests of the epoxy microcomposites which were simulated and studied by applying the finite element modeling method. For further comparison and analysis of the difference between the scratch behaviour of neat epoxy and epoxy microcomposites, the dimensions of the cuboid epoxy matrix and its constraints in this section were designed the same as those of the first design. Also, for control variable analysis, the friction coefficient between the matrix surface and the spherical indenter is 0.3 during this designed test which is the same as the first design. Furthermore, the main purpose of the second design is to study the effects of particle type, concentration and its filling position on epoxy microcomposites. The strengthening effect of soft rubber and hard silica particles on epoxy matrix was studied by increasing the volume fraction of both particles in equal proportion from 6% to 18% . The size of particles are

designed with three dimensions which are 2,6 and 10µm, and then the effect of particle size on epoxy microcomposite was studied. In the end, the influence of particle position on epoxy micro-composite was also investigated by filling the particles at positions of 6, 24 and 48µm underneath the surface. In order to avoid the influence of temperature and velocity on the simulation results, the simulated environmental conditions were assumed to be isothermal.

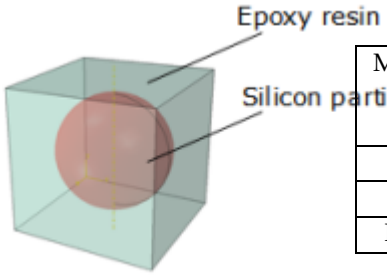

composites

Materials	Density (tonne/mm^3)	Young's Modulus (GPa)	Poisson's Ratio
Epoxy	2.25e-006	3	0.32
Silica	-	75	0.17
Rubber	-	0.25	0.45

Materials	Yield Stress (MPa)	Strain Hardening Modulus
Epoxy	80	100
Silica	1500	-
Rubber	-	-

3.2.3 Simulation models

(1) Spherical particle model

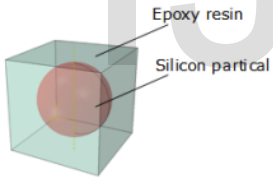

Figure 6 RVE model of micro particle i.e silica

The RVE with spherical inclusions is shown in above figure. Firstly, RVE is a method used to characterize the composition of the smallest unit of a microscopic model. Representative volume elements embedded with spherical inclusions are used to simulate polymer microcomposites. Also, RVE is the minimum volume that can be measured to evaluate micro model parameters and the size of the RVE is calculated based on the particle size and volume concentration.

(2) Indenter geometry

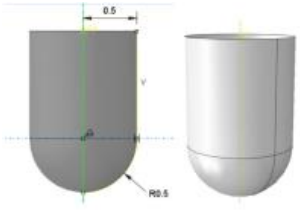

Figure 7 Spherical indenter geometry

Since the emphasis of the second design was not to study the influence of the indenter geometry on the composite, thus only a rigid spherical indenter with diameter of 1mm and height of 1.5mm was used to scratch the epoxy microcomposite matrix. The influence of normal load on the scratch performance of rubber particle reinforced epoxy microcomposite was studied by applying 5N and 20N normal load to the spherical indenter. The scratching velocity of the spherical indenter was set as constant 6m/s.

(3) Particles with different concentrations

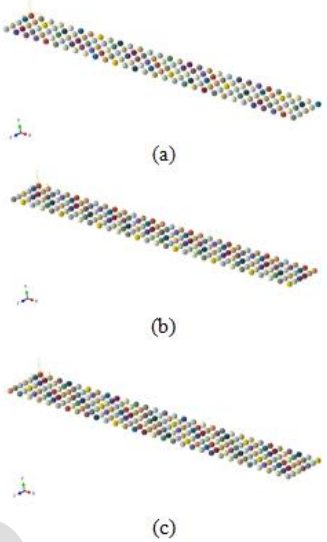

Figure 8 Rubber/silica particle with volume fraction of (a)6%,(b)12% and (c)18%

(4) Grid of models

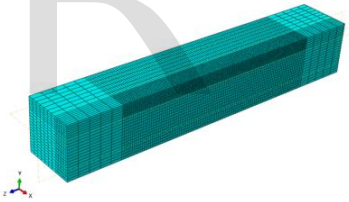

Figure 9 Matrix grid

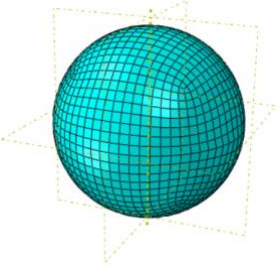

Figure 10 Particle grid

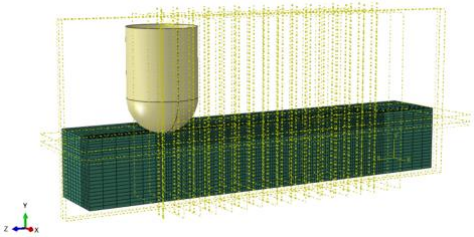

Figure 11 Assembly grid

3.3 Design Three: Wear test of rubber modified polymer microcomposites

3.3.1 Design requirements and aims

The third design is related to the wear test of rubber particles reinforced epoxy micro-composite. Also, the wear test is defined as the sliding friction under the condition of direct contact between the friction pair and the surface of the grinding material without any medium lubricating surface cleaning. Furthermore, the aim for the third design is to investigate the friction and wear properties of epoxy micro-composite materials filled with different volume fractions of micro rubber particles at four loads which are much higher than that of previous two designs. However, in order to easily derive the friction force used to calculate the friction coefficient and intuitively observe the difference of wear mass loss at different conditions, only two-dimensional finite element modeling was carried out for epoxy micro-composites. In addition, the same spherical indenter was used as in the second design and its scratch speed was set as 0.5 m/s. Since this part was designed to conduct two-dimensional finite element analysis on wear performance of epoxy micro-composites, the size of the rectangular epoxy matrix was 3x6 mm. The material properties of the epoxy matrix and particles were similar to those before but only the epoxy micro-composites filled with rubber particles was studied in this designed test.

The scratch test consisted of the three steps of indentation, scratching and rebounding was carried out several times uni-directional, but the wear test was conducted repeatedly bidirectional. Since the wear test was simulated to understand the effect of loads on the wear performance of epoxy/rubber micro-composites, high loads from 30N to 120N were applied normally at the centre of the spherical indenter to understand the variation of friction force, and then the friction coefficient can be calculated and plotted as the curves against the time. Furthermore, the total test time was extended to 5 minutes to carried out thousands of wear processes for more accurate calculation of the wear mass loss due to that the wear depth is related to the wear mass loss and its change was non-significant in a short test time.

3.3.2 Material properties

Table 4 Material properties of epoxy/rubber microcomposites

Materials	Density (tonne/mm^3)	Young's Modulus (GPa)	Poisson's Ratio
Epoxy	2.25e-006	3	0.32
Rubber	-	0.25	0.45

Materials	Yield Stress (MPa)	Strain Hardening Modulus
Epoxy	80	100
Rubber	-	-

3.3.3 Simulation models

(1) Establishment of two-dimensional model

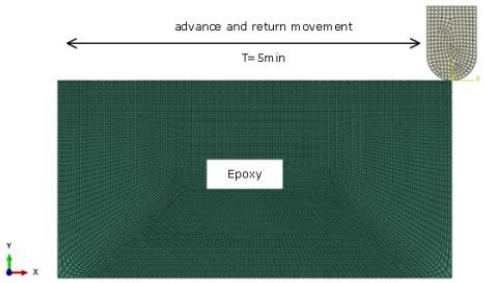

Figure 12 Basic simulation model for wear test of epoxy microcomposite

(2) Rubber particles with different concentrations

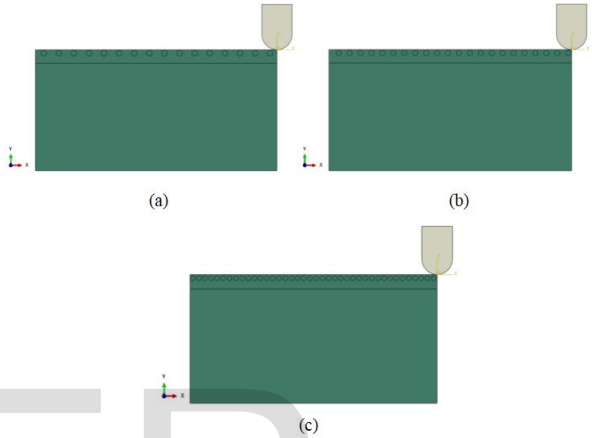

Figure 13 Rubber particle with volume fraction of (a)5%,(b)12.5% and (c)15%

(3) Friction output

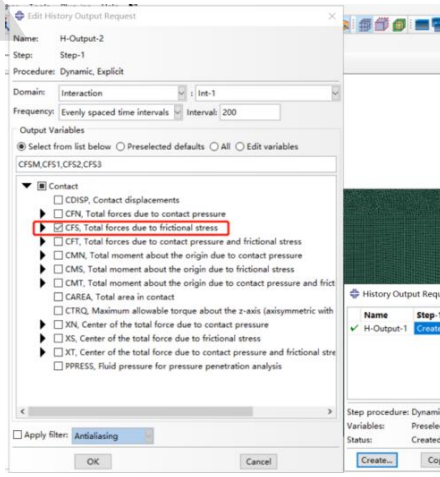

Figure 14 Extract the data of friction forces

Formula 1: Calculation of friction coefficient

$$\mu = \frac{Load}{Friction}$$

(4) Sketch map of wear mass loss

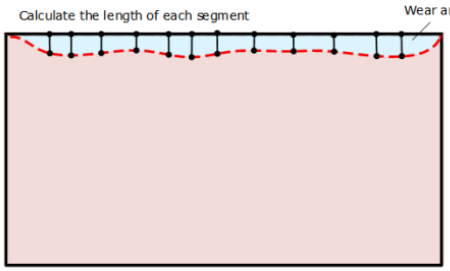

Figure 15 Wear area of epoxy micro-composites

Formula 2: Calculation of wear mass loss

$$WML(2D) = weardepth \times density$$

The numerical results of friction simulation were extracted according to the step shown in Figure 14, and the instantaneous friction coefficient value corresponding to each test time was obtained by applying the friction coefficient formula as shown above for relevant calculation, and a numerical plot was drawn for comparison and analysis. Also, for this part of the two-dimensional finite element analysis model, the wear mass loss can be measured by segmenting the wear depth corresponding to each test time as shown in Figure 15, thus to calculate the instantaneous wear mass loss and make a broken line graph for analysis and discussion.

CHAPTER IV: SIMULATION RESULTS AND DISCUSSION

4.1 Indentation and scratch test of single-phase polymer

4.1.1 Von Mises stress

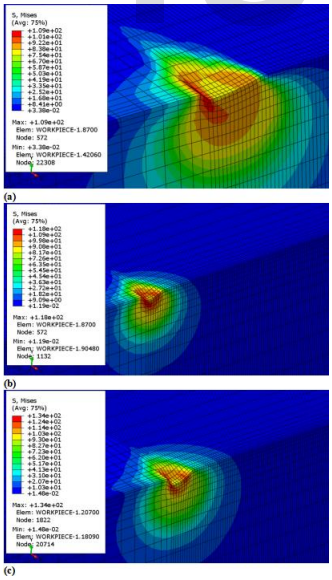

Figure 16 von Mises stress contour plot of epoxy matrix in the indentation test

In this part, the three von Mises stress contour plots from Figure 16 (a) to (c) are obtained by the indentation test of the spherical indenter, blunt and sharp conical indenter on the epoxy matrix respectively. By comparing the three plots, it can be found that when the high normal load is applied at a constant 20N, the use of sharp conical indenter will lead to the highest von Mises stress of 134MPa in the pure epoxy matrix, while the lowest von Mises stress of 109MPa in the process of using the spherical indenter to indent the pure epoxy matrix. The von Mises stress resulting from the indentation of an epoxy matrix with a blunt conical indenter is higher than that of a spherical indenter but lower than that of a sharp conical indenter. Therefore, it can be clearly seen that the von Mises stress on the surface of epoxy matrix increases with the increase of the indenter sharpness, and the indenter sharpness is in direct proportion to the von Mises stress magnitude.

By comparing plot (a) and plot (b), it can be found that the von Mises stress of the epoxy matrix increased from 109MPa to 9MPa as the spherical indenter was replaced by a blunt conical indenter with an angle of 120 ° at the tip. By comparing plot (b) and plot (c), it can be seen that when the blunt conical indenter is replaced by a sharp conical indenter with an Angle of 60 degrees at the tip, the von Mises stress on the epoxy matrix increases by 16MPa from 118MPa. It can be concluded that the more sharp the tip is, the greater the increase rate of von Mises stress in epoxy matrix is. In other words, the more sensitive von Mises stress is to the change of the indenter sharpness.

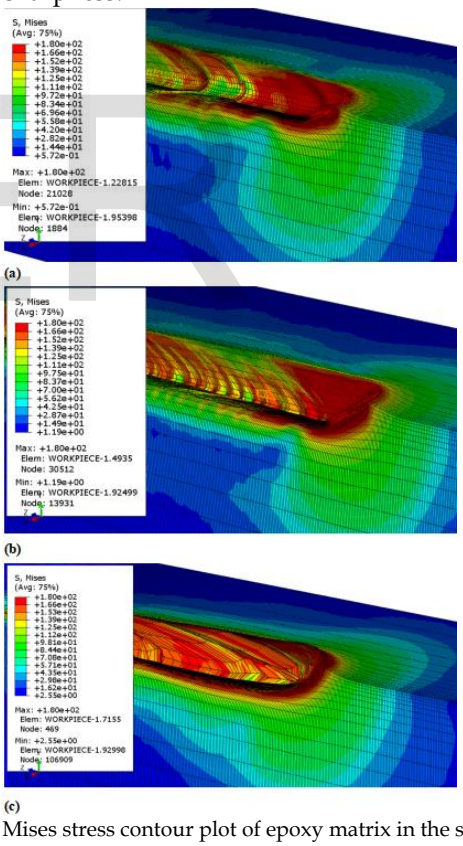

Figure 17 von Mises stress contour plot of epoxy matrix in the scratch test

The von Mises stress contour plots caused by the scratching of the spherical, blunt and sharp conical indenter on the epoxy matrix is described in Figure 17 from (a) to (c). By comparing the numerical results, it can be found that the von Mises stress magnitude of the epoxy matrix is almost the same at different conditions. However, the stress profile shown in the grid area of the figure indicates the maximum range of high von Mises stress caused by scratching the epoxy matrix with a sharp con-

ical indenter with an angle of 60 ° at the tip, followed by a blunt conical indenter with an angle of 120 ° at the tip. In addition, the magnitude of von Mises stress caused by the scratching of the indenter with three geometric shapes on the epoxy matrix varies throughout the scratch process, but the dark red area at the end of the scratch shown in the figure indicates that the magnitude of von Mises stress is the largest at the end of the scratch process. This phenomenon may be caused by material removal and slippage of the indenter during the scratching process, which affects the contact area between the scratching tip and the material. It was observed that the sharp conical indenter had a relatively small contact area with the epoxy matrix and caused the epoxy matrix to have a deeper scratch depth, which resulted in more severe material removal in the epoxy matrix. Moreover, the numerical results range of von mises stress caused by the scratching of the spherical indenter on the epoxy matrix from 0.572MPa to 180MPa is the largest of the three indenters. The maximum contact area between the spherical indenter and the material surface may be the cause of the extremely uneven distribution of von Mises stress. By comparing the simulation results of indentation and scratch test, it can be found that the von Mises stress of epoxy material during the scratch test is generally higher than that in the indentation test, but unlike the indentation test, there is no direct and clear relationship between the indenter sharpness and the von Mises stress magnitude.

4.1.2 Plastic Strain

Figure 18 shows the contour plot of plastic strain generated during the indentation process by (a) spherical indenter (b) blunt conical indenter and (c) sharp conical indenter by scratching the epoxy matrix. By observing the numerical results, it can be found that the plastic strain of the epoxy matrix caused by the sharp conical indenter is 0.646 which is the maximum, while the plastic strain of the epoxy matrix caused by the spherical indenter is 0.333, which is the minimum, about half of that caused by the sharp conical indenter. The plastic strain of the epoxy matrix induced by the blunt conical indenter is 0.479, which is between that induced by spherical and sharp conical indenter.

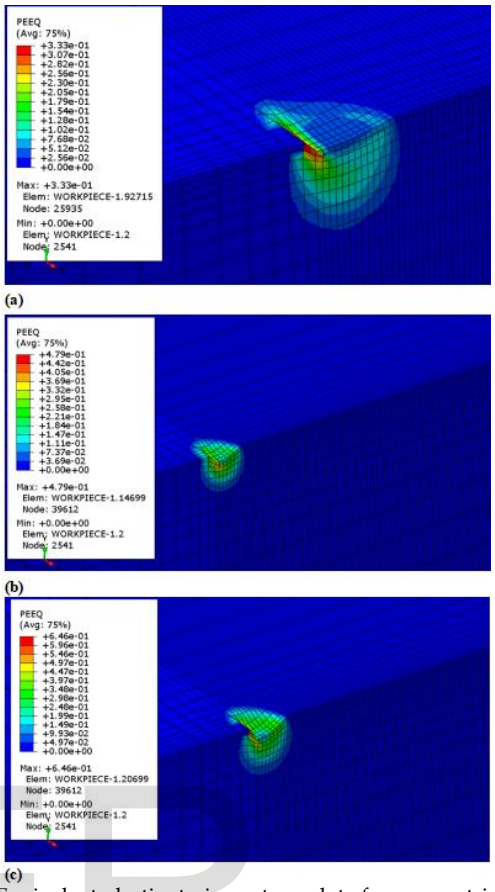

Figure 18 Equivalent plastic strain contour plot of epoxy matrix in the indentation test

The magnitude of the plastic strain usually represents the degree of the non-recoverable plastic deformation of the material, thus the non-recoverable damage caused by indentation of epoxy substrates with sharp conical indenter is more serious. By observing the deformation area in the Figure 18, it can be seen that the indentation depth of the epoxy matrix indentation caused by the spherical indenter is the shallowest, followed by the blunt conical indenter and sharp conical indenter results in the deepest indentation depth of epoxy matrix. This is due to the fact that the contact area between the tip of the sharp conical indenter and the material is minimal at the same applied normal load resulting in maximum plastic deformation.

Figure 19 describes the plastic strain contour plot of the epoxy matrix surface caused by (a) spherical indenter (b) blunt conical indenter and (c) sharp conical indenter during the scratch process. By observing the numerical results shown in the figure, it can be found that the plastic strain of the epoxy matrix caused by the spherical indenter is the minimum of 5.49. The plastic strain caused by scratching the epoxy matrix with a blunt conical indenter is 38.8 which is much larger than that of the spherical indenter, but close to 39.1 which is the maximum plastic strain of the sharp conical indenter. By comparison, it can be found that the range of plastic strain values caused by the spherical indenter is the smallest. Therefore, as previously assumed, the spherical indenter only induces sim-

ple scratch damage mechanism on the surface of epoxy matrix and low scratch visibility.

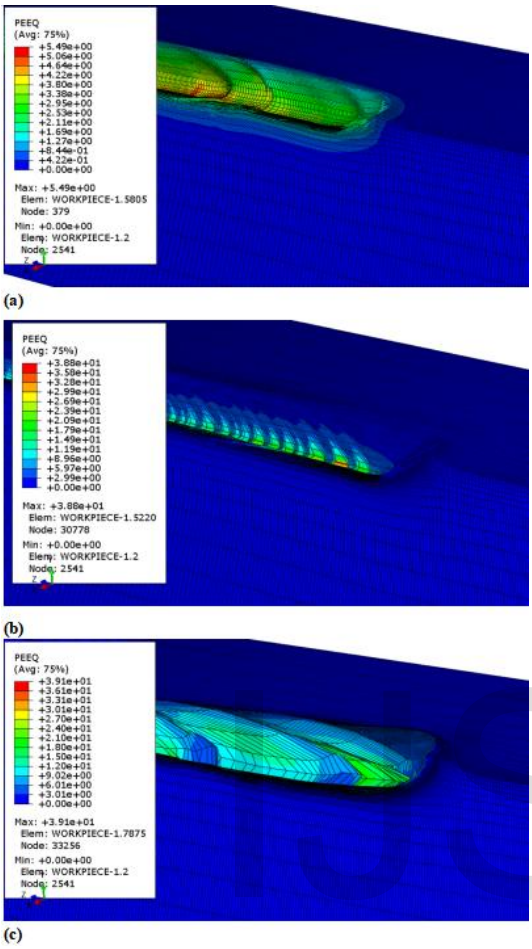

Figure 19 Equivalent plastic strain contour plot of epoxy matrix in the scratch test

However, the range of plastic strain values induced by the two conical indenters is much larger, leading to the possibility of relatively complex scratch damage patterns on the material surface and that induced by sharp conical indenters is the most serious. By observing the plastic strain profile of the epoxy matrix scratched with a blunt cone, clear and neat fish scale cracks were found on the surface of the epoxy matrix. However, it was found from plot (c) that scratching the epoxy matrix with a sharp conical indenter may cause the appearance of visible fracture layers and severe material removal on the epoxy matrix surface.

4.1.3 Maximal Principal Stress

In Figure 20, three maximum principal stress contour plot from top to bottom are obtained by indentation of spherical indenter, blunt indenter and sharp conical indenter on epoxy matrix in turn. As shown in the figure, since the indenters press along the direction perpendicular to the rectangular epoxy matrix, the maximum principal tensile stress and the maximum principal compressive stress exist along the direction of the indentation. The red region mainly represents the distribution of tensile stress, while the green and blue regions mainly represent the distribution of compressive stress. According to the observation of the three plots, the maximum principal tensile stress caused by the indentation of the spherical indenter on the epoxy matrix surface is 53.1MPa, and the maximum principal compressive stress is 158MPa. The maximum principal tensile stress caused by the blunt conical indenter indenting on the epoxy matrix surface of is 65.6MPa, and the maximum principal compressive stress is 273MPa. The maximum principal tensile stress on the epoxy matrix surface caused by the indentation of sharp conical indenter was 96.4mpa and 416MPa respectively. By comparing the numerical results, it can be found that the magnitude of the maximum principal tensile stress and the maximum principal compressive stress caused by the indentation of spherical indenter on the epoxy matrix is the lowest and that induced by the blunt conical indenter is higher than that induced by the spherical indenter. The maximum principal stress induced by the indentation of sharp conical indenter on the epoxy matrix is the highest, thus it can be concluded that at the same conditions, the magnitude of the maximum principal stress increases with the increase of the indenter sharpness, that is the indenter sharpness is in direct proportion to the magnitude of maximum principal stress.

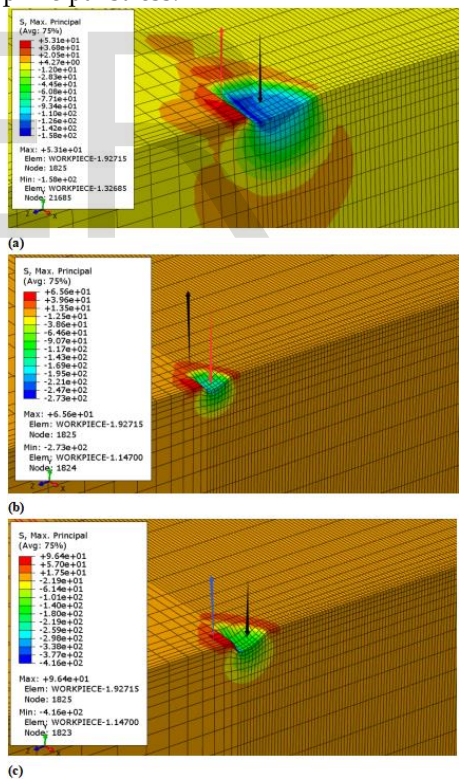

Figure 20 Maximum principal stress contour plot of epoxy matrix in the indentation test

By observing the stress distribution profile shown in the figure, it can be found that the maximum principal tensile stress caused by the three kinds of indentation is mainly distributed in the red region at the edge of the upper surface of the indentation groove, while the maximum principal compressive stress is mainly distributed in the blue region around the in-

denter tip inside the groove. The maximum principal tensile stress and the maximum principal compressive stress caused by the indentation of blunt conical indenter on the epoxy-matrix are 12.5mpa and 115MPa larger than that caused by the spherical indenter respectively, and the maximum principal tensile stress caused by the indentation of sharp conical indenter on the epoxy matrix increased by 30.8mpa and 143MPa respectively rather than that of blunt conical indenter. Therefore, it can be seen that the magnitude of the maximum principal tensile and compressive stress does not increase linearly with the increase of the indenter sharpness. Furthermore, if the indenter sharpness continues to increase, the growth rate of the magnitude of the maximum principal tensile and compressive stress will also increase.

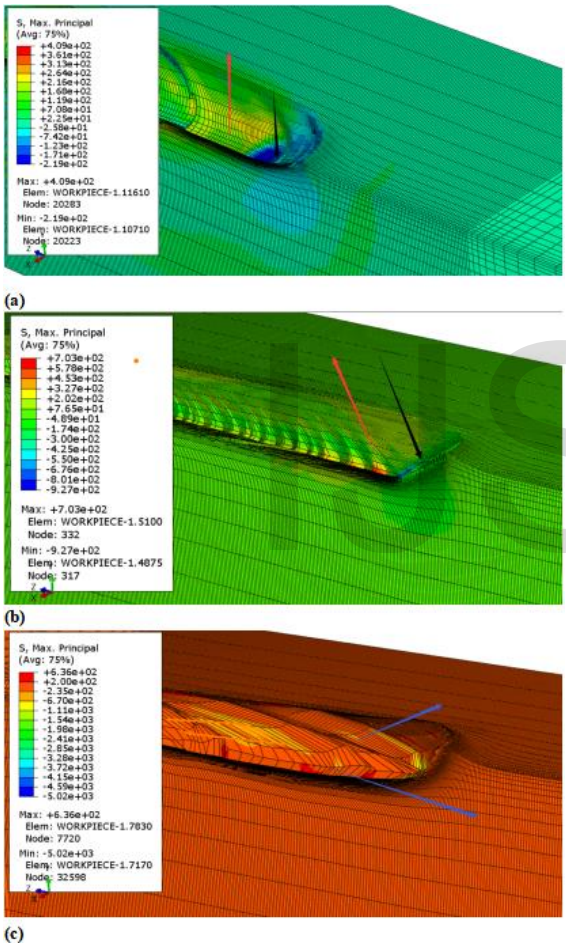

Figure 21 Maximum principal stress contour plot of epoxy matrix in the scratch test

The contour plot of the maximum principal stress generated by scratching the epoxy matrix with (a) spherical indenter (b) blunt conical indenter and (c) sharp conical indenter during the scratch process is described in Figure 21. By observing the numerical results, it can be found that the maximum principal tensile stress caused by the scratching of the spherical indenter on the epoxy matrix is 409MPa and the maximum principal compressive stress is 219MPa. Also, the maximum principal tensile and compressive stresses caused by scratching the epoxy matrix with a blunt conical indenter are 703MPa and 927MPa respectively. Furthermore, the maximum principal tensile and compressive stresses caused by scratching the epoxy matrix with sharp conical indenter are 636MPa and 5020MPa respectively. By comparing these numerical results, it can be seen that the maximum principal tensile stress of the epoxy matrix caused by the spherical indenter is the smallest, but the maximum principal tensile stress of the epoxy matrix caused by the blunt conical indenter is higher than that caused by the sharp conical indenter. Although the magnitude of the maximum principal tensile stress caused by the blunt conical indenter is the highest, the stress profile shown in plot (b) shows that the maximum principal tensile stress exists only in a few red regions before the end of the scratch process. However, as shown in plot (c), the maximum principal tensile stress caused by the sharp conical indenter is almost present in most of the notch positions, which indicates that the sharp conical indenter causes a large amount of elastic-plastic deformation on the epoxy matrix surface during the scratch process. Moreover, the magnitude of the maximum principal compressive stress of the epoxy matrix caused by the spherical indenter is also the lowest, but the magnitude of the maximum principal compressive stress caused by the spherical indenter and the blunt cone indenter is much lower than that caused by the sharp cone indenter. By analyzing the maximum principal stress contour plot of the epoxy matrix in the figure, it can be known that the maximum principal compressive stress is only distributed in a few blue regions before the end of the scratch process. As plot (c) shown, the maximum principal compressive stress of epoxy matrix caused by sharp conical indenter is not obvious but the magnitude is as high as 5020MPa, the reason for this phenomenon may be that the scratching of the sharp conical indenter results in the removal of a large amount of material from the epoxy matrix at the scratch site, which induces the contact area between the indenter and the material to be drastically reduced and causes the compressive stress to be temporarily concentrated in this tiny region below the scratch tip.

4.1.4 Scratch Depth

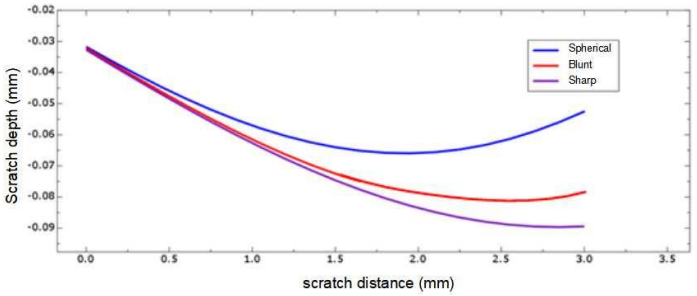

Figure 22 Scratch depth caused by three types of indenters versus scratch distance

Figure 22 shows the relationship between the scratch depths on the substrate surface caused by the spherical, blunt and sharp conical indenter and the scratch distance. At the beginning of the scratch process, as previously assumed, the depth of the scratch becomes deeper as the indentation sharpness increases, but subsequently the depth of the scratch caused by the spherical and blunt conical indentation is restored while the depth of the scratch caused by the sharp conical indentation is not. By observing the curve rising area of the scratch depth caused by the spherical indenter and the blunt conical indenter in this figure, it can be found that the scratch depth caused by these two types of indenter appears to recover from the scratch distance of about 2.25mm to the end. The reason for this phenomenon may be that the indenter with low sharpness accumulates part of the removal material in the scratch groove during the scratching process, which leads to the stick-slip phenomenon of the indenter and hinders the contact between the indenter tip and the inner surface of the groove. However, the non-recovery of the scratch depth caused by the sharp conical indenter is mainly due to the fact that the sharp indenter induces the material fracture during the scratch and the removed material does not accumulate in the scratch groove, thus the scratch depth becomes deeper and gradually reaches the critical value as the epoxy matrix is scratched by sharp conical indenter.

To sum up, the simulation results for the process of different geometric indenters indenting and scratching on the epoxy matrix surface are mainly analyzed in the first part. The blunter the indenter is, the shallower the scratch depth is and the more likely recovery is to occur. The sharper the indenter is, the deeper the scratch depth is and the greater the magnitude of the maximum principal compressive stress is. The geometry of the indenter not only affects the stress and strain distribution of the material surface but also determines the different damage mechanism such as fish scale and plowing cracks on the polymer surface.

4.2 Scratch test of polymer microcomposites

4.2.1 Effects of particle concentration and type

The influence of soft particle and hard particle concentration on the scratch behavior of multi-phase polymer system was studied by simulating epoxy/rubber micro-composites and epoxy/silicon dioxide micro-composites. Rubber and silica particles with particle size of 10 μm were filled into the epoxy matrix at volume fractions of 6, 12 and 18%, respectively, and the scratch behavior characteristics of the composite were discussed by comparing the simulation results of pure epoxy with the particle concentration of 0% in the first part.

4.2.1.1 Von Mises stress

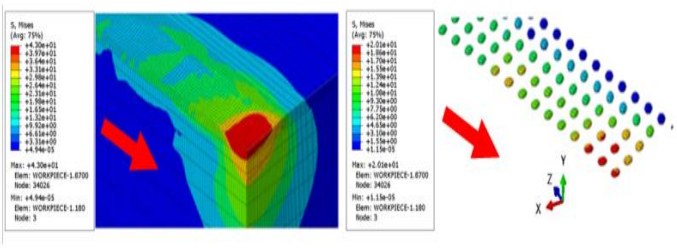

Figure 23 Von Mises stress contour plot of epoxy/ 6% rubber micro-composites at 5N

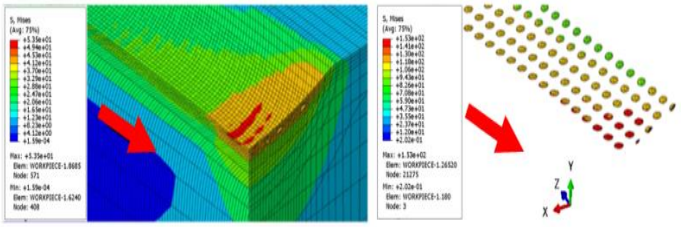

Figure 24 Von Mises stress contour plot of epoxy/ 6% rubber micro-composites at 20N

Figures 23 and 24 above show the von mises stress profiles of rubber particles and epoxy matrix at volume fraction of 6% when a small load of 5N and a large load of 20N are applied normally. To facilitate the analysis of the stress profile on the model surface, the indenter model is hidden and the contour plot mainly shows the von Mises stress on the model cross-section. It can be seen from Figure 23 that the von Mises stress on the epoxy matrix is higher than that on the soft rubber particles when the applied load is 5N, i.e. the load is relatively small. Instead, Figure 24 shows that the von Mises stress of the rubber particles is higher when the normal load is applied at 20N. Through analysis, it is concluded that the rubber particles are constrained by the influence of high Poisson's ratio of rubber and the plastic deformation of epoxy matrix, which results in the difference of von Mises stress in the two cases.

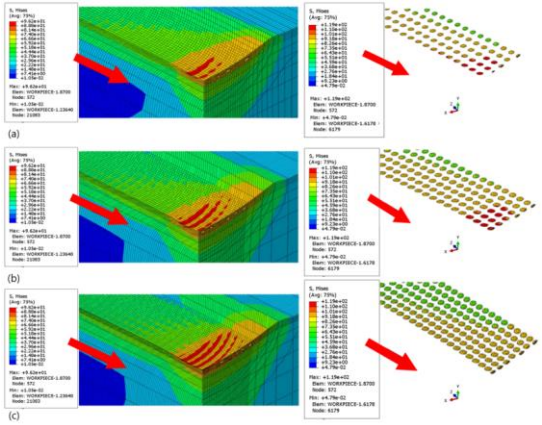

Figure 25 Von Mises stress contour plot of epoxy/ (a)6%,(b) 12%,(c) 18% rubber microcomposites at 20N

According to the above figure, it can be observed that at the same normal load conditions, the concentration of soft rubber particles is inversely proportional to the von Mises stress on the particles, and the increase of the concentration of soft par-

ticles will lead to the decrease of von Mises stress on the particles. On the contrary, the concentration of soft rubber particles is proportional to the von Mises stress in the epoxy matrix, and with the increase of the concentration of rubber particles, the von Mises stress in the epoxy matrix also increases.

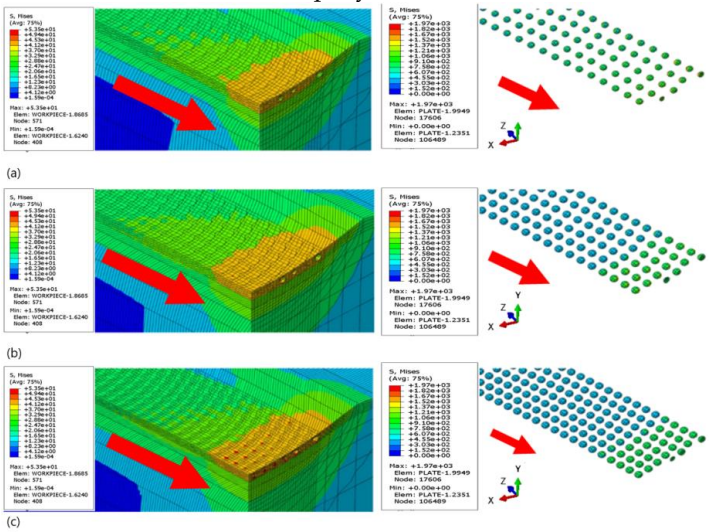

Figure 26 Von Mises stress contour plot of epoxy/ (a)6%,(b) 12%,(c) 18% silica microcomposites at 20N

Figure 26 describes the von Mises stress profile of the epoxy matrix modified by 6,12, 18% hard silica particles at 20N normal loading. Through observation, it can be found that the influence of the concentration of hard silica particles on the particles and the epoxy matrix is similar to that of soft rubber particles described in Figure 25, but the von Mises stress of the epoxy matrix is much lower than that of hard silica particles, which is different from that of soft particles. At the same normal load, the concentration of the two types of particles increase will make the von mises stress in epoxy matrix increases, it shows that the increase of particle concentration will make stress on material distribution more uniform, and the von mises stress of soft rubber particles is far lower than the same simulation conditions of hard particles, this kind of phenomenon is mainly due to the high rigidity of hard particles, thus to make the stress concentration in the particles.

4.2.1.2 Plastic strain

In the indentation and scratch simulation test, the epoxy matrix mainly shows elastic deformation and plastic deformation. In contrast, both soft and hard particles show only elastic deformation, thus the equivalent plastic strain of silica and rubber particles is not considered. Figure 27 describes the equivalent plastic strain contour plot of the epoxy microcomposite modified by rubber particles of different concentrations when a high load of 20N is applied.

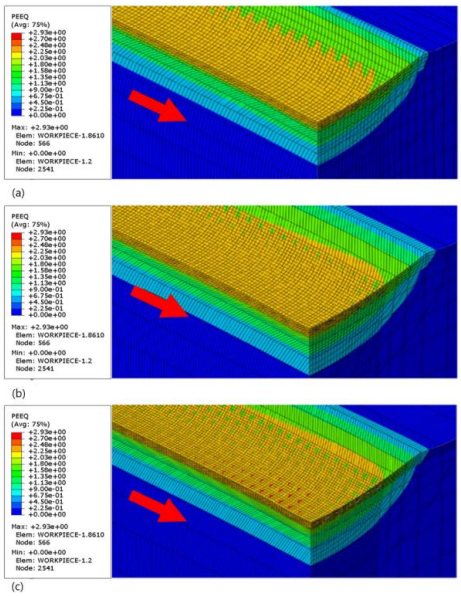

Figure 27 Equivalent plastic strain contour plot of epoxy/ (a)6%,(b) 12%,(c) 18% rubber microcomposites at 20 N

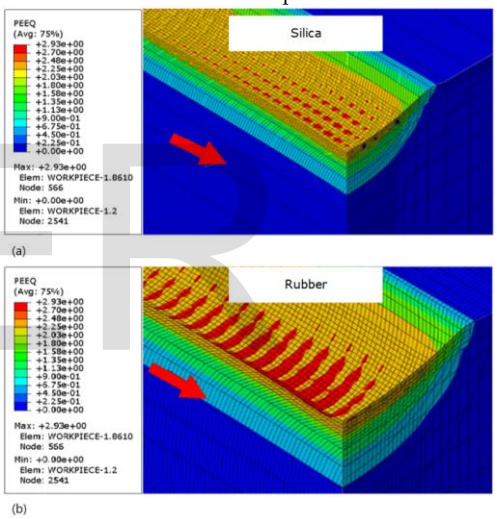

Figure 28 Equivalent plastic strain contour plot of (a) epoxy/ 6% rubber,(b) epoxy/ 6% silica microcomposites at 20 N

By analyzing Figure 27, it can be found that the plastic strain of the micro-composite is proportional to the concentration of rubber particles. When the particle concentration increases, the plastic strain of the composite increases and the residual scratch depth of the material surface also increases, which indicates that the compressive resistance of the composite is inversely proportional to the rubber particle concentration. The residual scratch depth represents the compression behavior of composites, and the deeper the residual scratch depth is, the worse the compressive performance of composites will be.

Figure 28 is the equivalent plastic strain contour plot of the soft and hard particle modified composite material with the same volume fraction at high load of 20N. The strain trends of hard silica particles and soft rubber particles reinforced epoxy composites are similar. However, it can be seen from the observation of Figure 28 that under the same conditions, the plastic strain of the epoxy composite reinforced by soft rubber particles is higher than that of the epoxy composite

reinforced by hard silica particles, which also explains why the residual scratch depth on the surface of the epoxy composite filled by soft particles is higher. The simulation results show that the increase of the volume fraction of soft particles decreases the compression performance of epoxy composites, while the increase of the concentration of hard particles improves the compression performance of epoxy composites.

4.2.1.3 Maximum principal stress

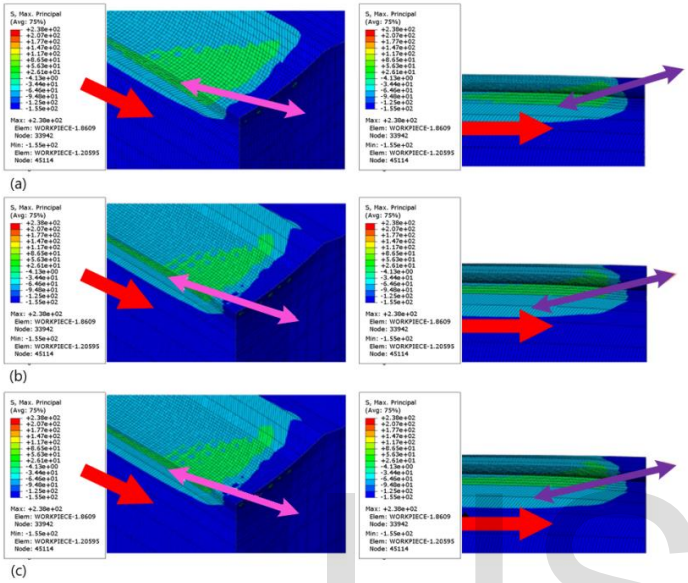

Figure 29 Maximum principal tensile stress contour plot of epoxy/ (a)6%,(b) 12%,(c) 18% rubber microcomposites at 20N

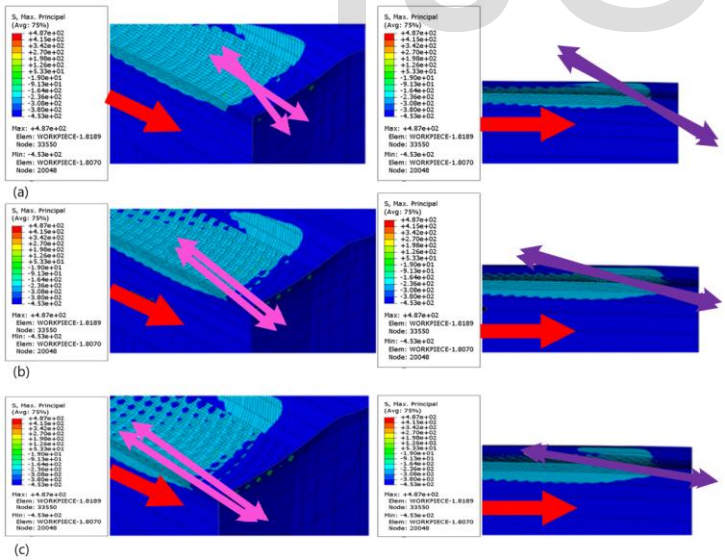

Figure 30 Maximum principal tensile stress contour plot of epoxy/ (a)6%,(b) 12%,(c) 18% silica microcomposites at 20N

The maximum principal tensile stress is the vector sum of normal stress and shear stress and its magnitude and direction are obtained by analyzing the magnitude and direction of the maximum principal compressive stress and the maximum principal tensile stress. Therefore, the maximum principal stress is used to describe the actual stress of the structure, and its magnitude determines whether cracks and shear failure occur in the structure. The direction is the direction of the actual failure surface. In this simulated scratch test, the occurrence, formation and type of microcracks are mainly determined by the direction and magnitude of the maximum principal tensile stress behind the scratch tip. Also, Figure 29 depicts the contours of the maximum two-dimensional principal tensile stress of the epoxy composite modified by pure epoxy material and 6%, 12%, 18% volume fraction rubber particles at a normal load of 20N. Furthermore, Figure 30 shows the contour map of the maximum two-dimensional principal tensile stress of pure epoxy material and the composite modified by silica with different concentrations at 20N normal load.

By comparing and analyzing the simulation results of epoxy microcomposite model in Figure 29 and Figure 30, the tensile model of single epoxy cracking is explained. Figure 29 shows that the maximum principal tensile stress direction of the multi-phase epoxy microcomposite is out of plane and that the cracking mode of the epoxy composite containing soft rubber particles is mixed. In relevant experiments, the mixing cracking direction is usually perpendicular to the direction of the maximum principal tensile stress [46]. In Figure 30, the maximum principal tensile stress direction of the epoxy composite modified by hard silica particles is also similar to that of the epoxy composite modified by soft rubber particles in Figure 29. According to the above simulation results, the maximum principal tensile stress direction of epoxy composites containing only soft rubber particles does not change with the modification of soft particle concentration. As shown in Figure 30, the maximum principal tensile stress direction of the epoxy composite containing hard silica particles gradually changes from the outside to the inside with the increase of particle concentration. However, the change of the concentration of hard and soft particles will not have a great influence on the magnitude of the maximum principal tensile stress. Moreover, it is different from the epoxy composite containing soft rubber that the change of the maximum principal stress direction of the epoxy composite modified by different concentration of hard silica particles indicates that the cracking mode of the composite surface gradually changes from the mixed form to the tensile mode.

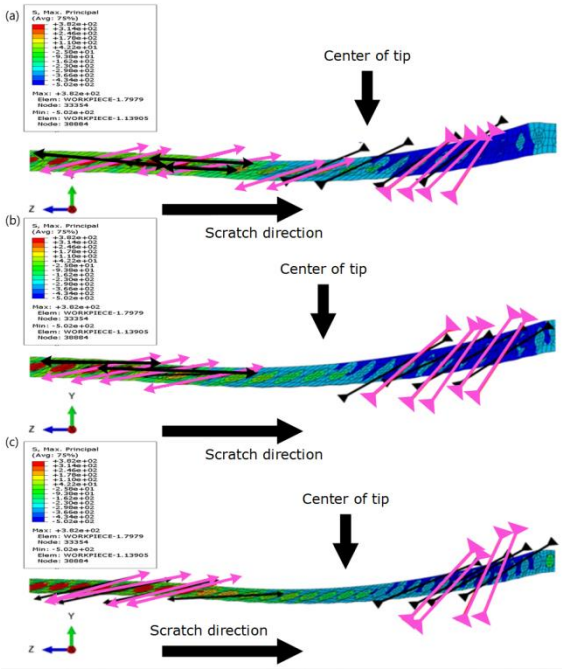

Figure 31 Maximum principal stress contour plot of epoxy/ (a)6%,(b) 12%,(c) 18% rubber microcomposites at 20N

Figure 31 depicts the two-dimensional contour plot of the maximum principal stress of epoxy composites containing soft rubber particles of different concentrations at 20N normal load. In Figure 31, the direction of the maximum principal tensile stress is represented by an arrow pointing outwards and the direction of the maximum principal compressive stress is represented by an arrow pointing inwards. The black arrow and pink arrow indicate the direction of maximum principal stress of epoxy matrix and soft rubber particles respectively. By analyzing the figure, it can be seen that the compressive stress mainly exists below the scratch tip and the tensile stress mainly exists behind the scratch tip. When the volume fraction of soft rubber particles increases, the direction of the maximum tensile stress of the particles and the epoxy matrix is similar. In the same situation as that of soft rubber particles, the direction of maximum principal tensile stress on the matrix of epoxy composite modified by hard silica particles tends to be the same as that on the particle with the increase of the particle volume fraction. Therefore, the increase of the concentration of both soft and hard particles will make the strain between the epoxy matrix and the particles match better. Furthermore, the surface debonding of multi-phase polymer is a prerequisite for micro-crack generation. With the increase of particle volume fraction, the possibility of debonding the material behind the tip of the indenter in the surface scratching process of multi-phase polymer is greatly reduced. In this simulated scratch test, the magnitude of the maximum principal compressive stress in the area below the scratch tip is much smaller than that behind the scratch tip, and the direction of the maximum principal compressive stress is almost unchanged.

4.2.2 Influence of particle size

Three kinds of hard and soft particles with different particle sizes modified epoxy matrix were used to study the influence of particle size on the scratch behavior of epoxy composites. In order to improve the efficiency of simulation, the particle concentration is designed as 0.5%.

4.2.2.1 Maximum principal stress

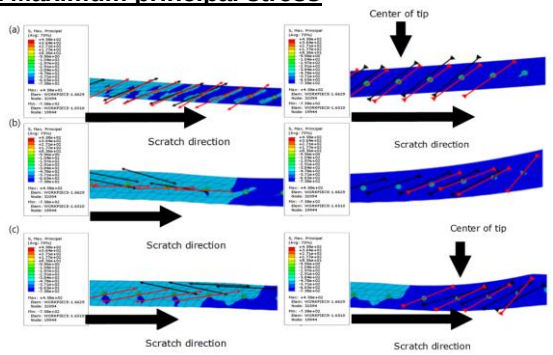

Figure 32 Maximum principal stress contour plot of epoxy/ (a)2,(b) 6,(c) 10 µm silica particles microcomposites at 10N

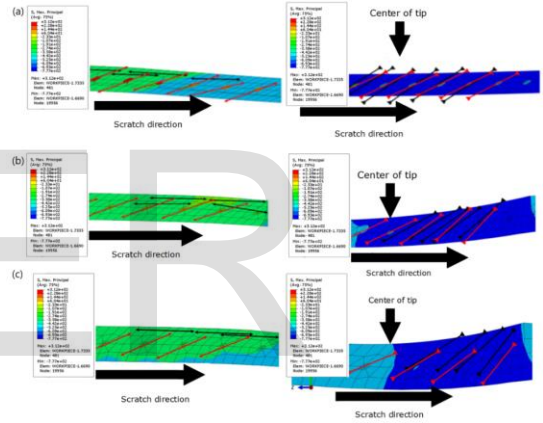

Figure 33 Maximum principal stress contour plot of epoxy/ (a)2,(b) 6,(c) 10 µm rubber particles microcomposites at 10N

Figure 32 depicts the maximum principal stress contour plots of 2,6,10 µm diameter hard silica particles modified epoxy composite at a 10N load. Figure 33 shows the maximum principal stress contour maps of 2,6,10 µm soft rubber particle modified epoxy composite at a 10N normal load.

By analyzing the finite element simulation results in Figure 32 and 33, when the particle size of soft rubber decreases, the magnitude of the maximum principal tensile stress existing behind the scratch tip also decreases, which will lead to the delay of cracking on the surface of epoxy composite reinforced by rubber particles. However, the change of hard silica particle size can not affect the maximum principal tensile stress and surface cracking conditions of the composite. As shown in the figure above, the direction of the maximum principal tensile stress is indicated by an outward arrow and the direction of the maximum principal compressive stress is indicated by an inward arrow. Black and red arrows represent the maximum principal stress directions of the epoxy matrix and the particle respectively. Through observation, it can be found that the maximum principal tensile stress and the maximum principal compressive stress exist behind and below the scratch tip re-

spectively. The modification of soft rubber particle size has no effect on the maximum principal stress of rubber modified epoxy composite. In contrast, with the decrease of the size of hard silica particles, the stress between the particles and the epoxy matrix is more compatible, which also leads to the decrease of the possibility of decohesion on the surface of silica particles reinforced epoxy microcomposite.

4.2.3 Influence of particle position underneath the surface

4.2.3.1 Von Mises stress

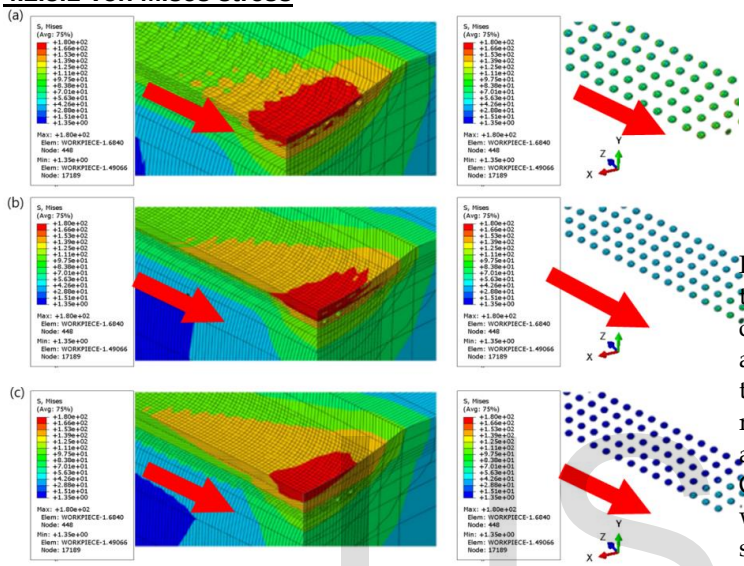

Figure 34 Von Mises stress contour plot of epoxy microcomposites at 20N with silica particles filled at positions (a) 6, (b) 24, (c) 48 μm underneath its surface

Figure 34 describes the von Mises stress distribution of the epoxy microcomposite modified by silica particles at different filling positions when the applied normal load is 20N. The von Mises stress of epoxy microcomposites is higher the closer the silica particles are located to the material surface, although it is difficult to detect the difference in the stress of epoxy microcomposites caused by different particle positions through direct observation. The relationship between the position of soft rubber particles from the material surface and the von Mises stress of epoxy microcomposites is similar, which also indicates that the closer the epoxy matrix is to the material surface with the distribution of particles, the more plastic deformation will occur during the scratch process.

4.2.3.2Maximum principal stress

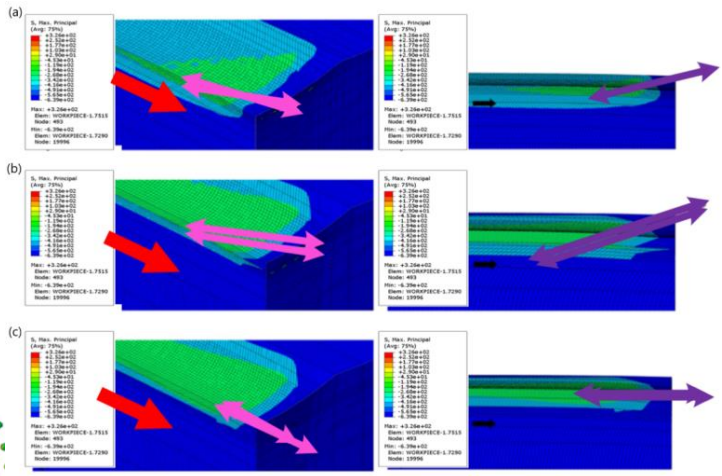

Figure 35 Maximum principal tensile stress contour plot of epoxy microcomposites at 20N with rubber particles filled at positions (a) 6, (b) 24, (c) 48 μm underneath its surface

Figure 35 depicts the maximum principal tensile stress contour plot of epoxy microcomposites modified by rubber particles with different filling positions at a normal load of 20N. By analyzing the figure, it can be seen that the closer the distribution position of soft rubber particles is to the surface of the micro-composite, the greater the possibility of mixing cracking appears behind the scratch tip on the surface of the composite. On the contrary, the rubber-modified epoxy microcomposite will behave like a pure matrix as the distribution position of soft rubber particles tends to be further from the surface of the micro-composite. The magnitude of the maximum principal tensile stress that exists behind the scratch tip cannot be affected by changes in the distance between the two particles to the epoxy microcomposite surface, but the direction of the maximum principal tensile stress will gradually change inward as the particle position gets closer to the material surface, resulting in the mixed cracking mode behind the scratch tip.

To sum up, the scratch and tribological behavior of multi-phase polymer were deeply understood through finite element simulation of scratch test of rubber and silica particles modified epoxy microcomposite. The simulation results in the second part show that the filling particles have a significant effect on the stress-strain field of the micro-composites. Also, the increase of the volume fraction of hard and soft particles will result in large plastic deformation on the surface of the material. By comparison, it is found that the surface of epoxy microcomposites modified by hard particles has relatively low plastic strain, thus the residual scratch depth on the surface of the epoxy microcomposites is shallower. In addition, the decrease of particle size will delay the surface cracking of rubber-modified epoxy microcomposite and the closer the particle position is to the surface, the more complex damage mechanism will appear on the surface. In conclusion, numerical simulation using finite element modeling method can intuitively show the scratch damage evolution process of multi-phase polymer materials.

4.3 Wear test of polymer microcomposites

4.3.1 Effects of load on the wear properties of polymer and its microcomposites

4.3.1.1 Friction coefficient

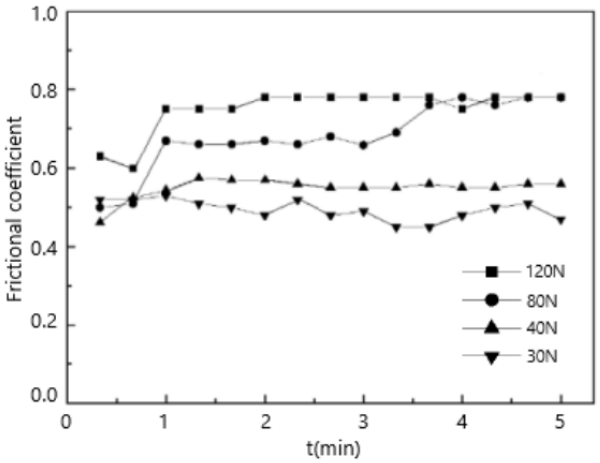

Figure 36 Effect of load on friction coefficient of pure epoxy

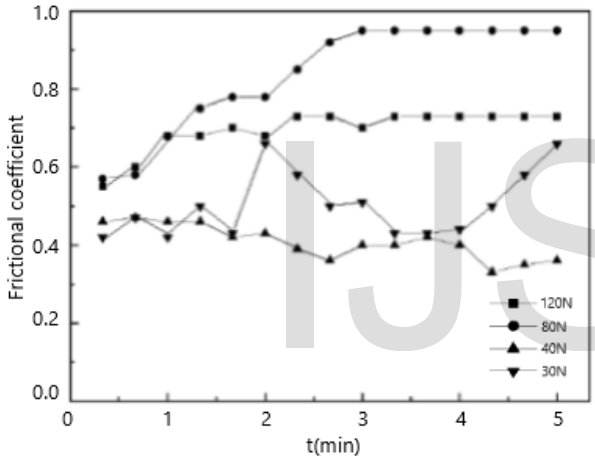

Figure 37 Effect of load on friction coefficient of epoxy/ 5%rubber microcomposite

Figure 36 shows the variation of the friction coefficient of the pure epoxy matrix at different normal loads. By analyzing the above figure, it can be found that the friction coefficient value of epoxy matrix fluctuates around 0.5 and cannot change significantly at relatively low loads such as 30N and 40N. However, when the applied normal load increases to 80N, the friction coefficient tends to rise and the average friction coefficient reaches about 0.7. As the load continues to increase to 120N, the friction coefficient also increases to about 0.78. By comparing the curve plots, it can be seen that the friction coefficient increases with the increase of the normal load and the friction coefficient is in direct proportion to the normal load. During the simulation of wear test, the wear of the material mainly comes from the transfer of the material to the dual surface of the friction pair. The increase of normal load will increase the frictional tangential force, which will aggravate the wear of the material surface by the spherical indenter, increase the material transfer to the dual surface, and increase the adhesive wear. Due to the high brittleness of the pure epoxy matrix, fatigue wear occurs which is a major wear pattern of epoxy resin when sliding on a hard dual surface and the surface roughness of the material increases which makes the friction coefficient between the material and the friction pair also increases.

Figure 37 describes the variation of friction coefficient of rubber-reinforced epoxy microcomposites with a particle content of 5% at increasing normal loads. By comparing the friction coefficient curves based on the simulated data in Figure 37 and Figure 36, the friction coefficient of epoxy/5% rubber micro-composite material fluctuates more violently at a lower normal load. The reason for this status is that no more effective transfer film is formed at 30N and 40N normal loads, so the friction coefficient is unstable. However, at higher normal loads of 80N and 120N, rubber particles debond due to increased friction between the tip of the indenter and the material surface, which increases the surface roughness and leads to a sharp increase in the friction coefficient. When 120N normal load is applied, the more abrasive debris generated by wear makes the transfer film thicker and more self-lubricating. Therefore, in the case of 120N normal load, the surface friction coefficient of the micro-composite material is less than that in the case of 80N load.

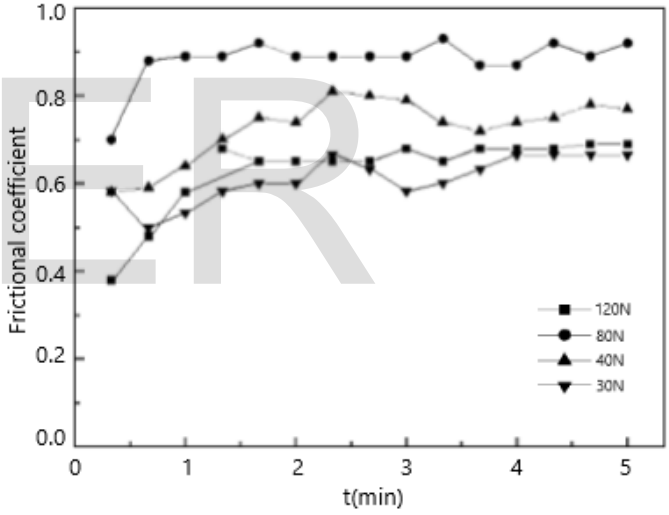

Figure 38 Effect of load on friction coefficient of epoxy/12.5% rubber microcomposite

Figure 38 shows the variation of the friction coefficient of epoxy microcomposite containing 12.5% volume fraction micro rubber particles at different normal loads. To compare with the results of neat epoxy shown in Figure 36, the epoxy microcomposite with 12.5% volume fraction rubber particles reinforced has a larger value of friction coefficient. Since rubber is a material with good ductility, when the rubber particles are filled into the epoxy matrix, the toughness of the epoxy matrix is also improved. The rubber particles are constantly exposed to the friction surface during the material wear test, thus the particles are subjected to a large amount of friction, which makes the friction coefficient of the epoxy microcomposite reinforced with 12.5% volume fraction rubber particles higher. By analyzing the Figure 38, it can be observed that the average friction coefficient is the highest at normal load of 80N

and lowest at normal load of 30N. Also, the coefficient of friction at normal load of 120N is only higher than that at 30N normal load and it is lower than both value at 40N and 80N which is totally different from the direct proportional relationship between the normal load and friction coefficient of neat epoxy. The phenomenon occurs due to the micro rubber particles are filled into the epoxy matrix which makes it easier for the material to form a transfer film that can effectively reduce the friction coefficient during wear process. Furthermore, when the applied normal loads are from 30N to 80N, the generation of transfer film is relatively small and the surface wear of the material is smaller. However, at 120N normal load, severe wear on the surface of the material leads to the generation of more transfer film with self-lubrication, thus the friction coefficient of the epoxy microcomposite is affected by the formation of transfer film to decrease.

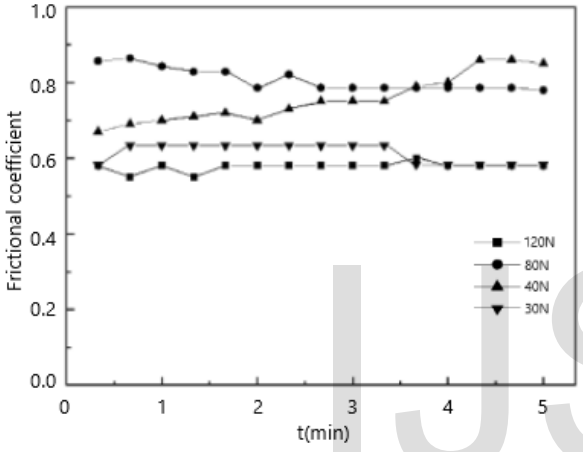

Figure 39 Effect of load on friction coefficient of epoxy/15% rubber microcomposite

In Figure 39, the effect of normal load on the friction coefficient of epoxy microcomposite containing 15% volume fraction micro rubber particles is similar to that of epoxy composite containing 12.5% volume fraction micro rubber particles. The epoxy microcomposites containing 15% rubber particles have the highest friction coefficient at 80N normal load and the lowest friction coefficient at 120N normal load. After 4 minutes of wear testing, the coefficient of friction at 80N normal load is less than that at 40N normal load and the coefficient of friction at 30N is greater than that at 120N which illustrates that the formation of transfer film at 80N effectively reduces the friction coefficient of material surface, thus the friction coefficient keeps stable within a constant range. When the applied normal load is 120N, the friction coefficient of epoxy microcomposite is the most stable. In the case of high normal load, the surface wear of the material intensifies and the temperature rises, resulting in the production of a large number of transfer films which can provide the good lubrication effect. Therefore, the friction coefficient of the micro-composite material is also the minimum at 120N load.

4.3.1.2 Wear mass loss

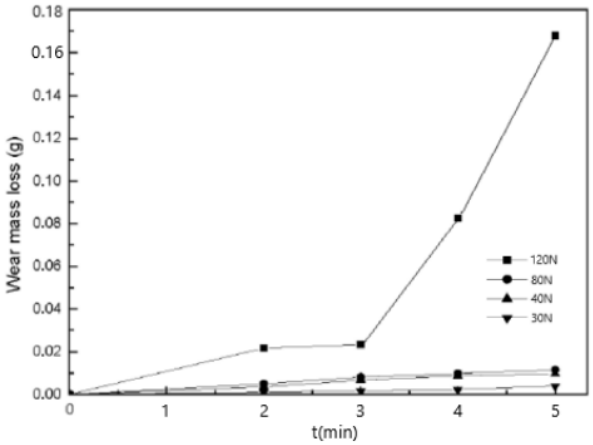

Figure 40 Effect of load on wear mass loss of neat epoxy matrix

By observing the wear mass loss curve in Figure 40, it can be seen that the wear mass of the pure epoxy matrix increases with the increase of normal load, thus the normal load is proportional to the wear mass of the pure epoxy material. When the applied normal loads are from 30N to 80N, the wear mass of epoxy matrix cannot change significantly and is much less than that of 120N. Compared with the case of 120N load, the wear mass loss of epoxy matrix increases linearly when applied with 30N to 80N. At the normal load of 120N, the loss of wear mass increases rapidly after 3 minutes of simulated wear test. The entire simulation process of the wear test lasted for 5 minutes, and the wear mass loss at 120N normal load before the end of the test was approximately 17 to 40 times that under the other three loads, thus the wear performance of the epoxy matrix at 120N load changed significantly. The reason for this phenomenon is that the surface of pure epoxy matrix cannot show plastic deformation when the normal load is equal to or less than 80N so that the friction coefficient increases linearly with the change of test time. Moreover, due to extensive plastic deformation on the surface of pure epoxy matrix at 120N load, the friction coefficient and wear mass loss increase. With the increase of the temperature of the wear position of the matrix surface, the plastic flow phenomenon occurs in the wear position, that is, the self-lubrication effect.

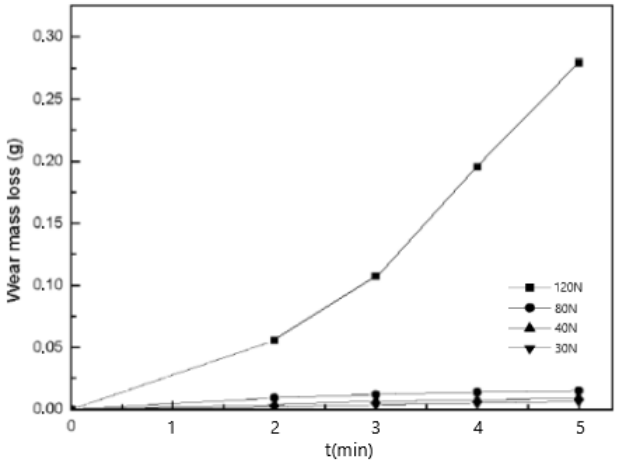

Figure 41 Effect of load on wear mass loss of epoxy/5% rubber microcomposite

As shown in Figure 41, for epoxy micro-composite reinforced with 5% micron rubber particles, the change in wear mass loss with increased load is similar to that of the previously pure epoxy matrix. However, compared with the pure epoxy material, the growth rate of wear mass loss of rubber-reinforced epoxy micro-composite decreased with time at120N normal load. Furthermore, at normal loads of 30N, 40N and 80N, the wear mass loss of epoxy micro-composite is very close and the trend is similar, but the wear mass loss of epoxy micro-composites is still much larger at 120N load than that at lower loads.

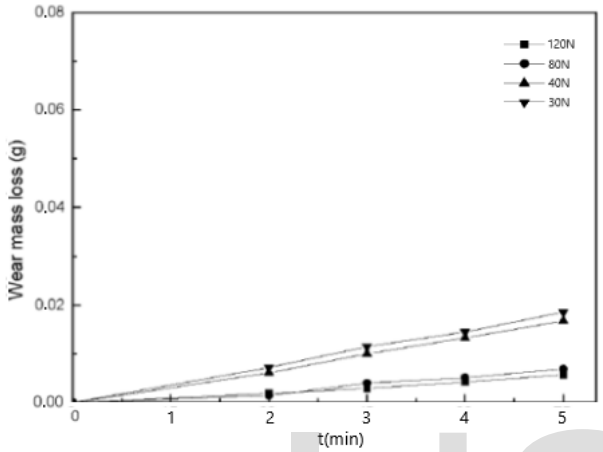

Figure 42 Effect of load on wear mass loss of epoxy/12.5% rubber microcomposite

Figure 42 describes the wear mass loss curve of 12.5% micro rubber particles reinforced epoxy microcomposite at four different loads. By observing the figure, it can be found that the wear mass loss of epoxy microcomposite at either normal loads cannot change significantly by filling the micro rubber particles. Also, the rubber particles improve the ductility of epoxy microcomposite to reduce the loss of wear mass even at high normal loads. By comparing the numerical results with previous that of pure epoxy and 5% micro rubber particles reinforced epoxy, it can be observed that the wear property of the micro-composite is greatly improved after filling 12.5% micro rubber particles.

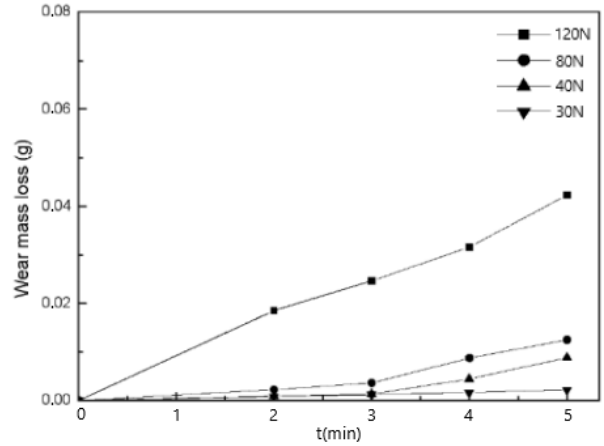

Figure 43 Effect of load on wear mass loss of epoxy/15% rubber microcomposite

In Figure 43, the wear mass loss of 15% micro rubber particles reinforced epoxy microcomposites varies with different load conditions are plotted. It can be seen that the wear mass loss of micro-composite is in direct proportion to the loads. When the applied normal load equals to and below 80 N, the difference in wear mass loss of micro-composite is not significant. By analyzing the numerical results, the wear mass loss of material at 120 N is about 4 to 30 times that at other three loads. Compared with the neat epoxy matrix, the wear performance of the microcomposites was greatly improved but slightly worse than that of the epoxy microcomposites reinforced with 12.5% rubber particles. Therefore, when the volume fraction of the filling particles increases to 15%, the wear mass loss of the material increases, that is, the wear resistance decreases.

4.3.2 Effect of rubber particles concentration on the wear property

4.3.2.1 Friction coefficient

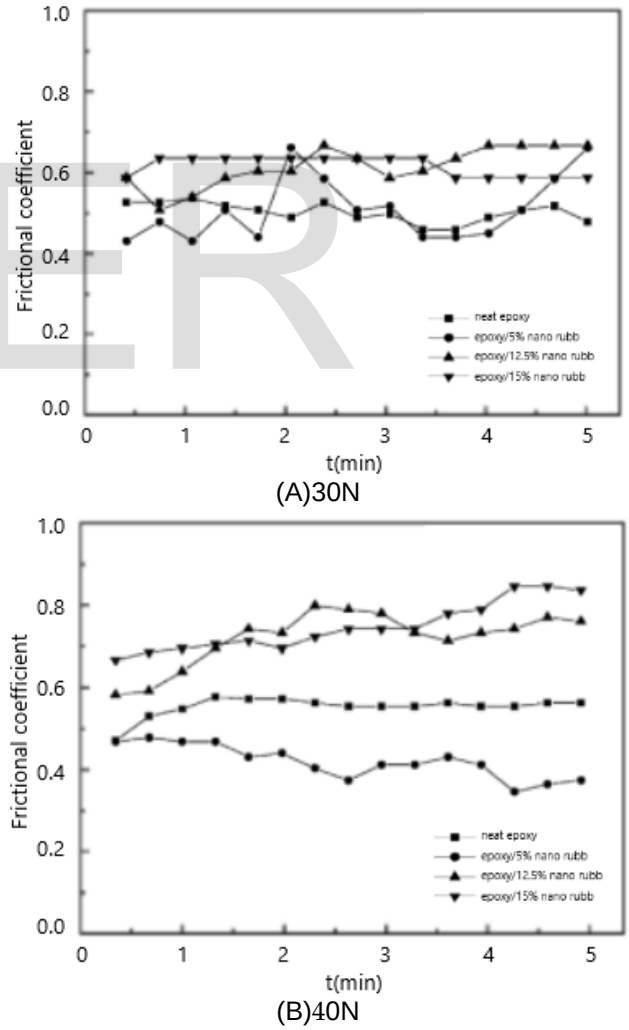

Figure 44 Effect of micro rubber concentration on friction coefficient of epoxy microcomposite (A-B).

Figure 44 (A) describes the variation curve of friction coefficient of epoxy microcomposite reinforced by rubber particles

at four different particle concentrations when the normal load is constant 30N. The friction coefficient of epoxy microcomposites containing 12.5% and 15% micron rubber was stable by observation. In comparison, the friction coefficient of epoxy microcomposite material containing 5% micron rubber fluctuates greatly. Also, when the applied normal load is 30N, the micro-composites bear less shear stress and produce less heat on the surface. Furthermore, at lower normal loads, the surface of epoxy microcomposite does not crack and its surface roughness does not change significantly, thus the friction coefficient is small. In the case of slight wear, the surface of the material is less abrasive, for example, the surface of epoxy microcomposite reinforced with 5% concentration of micron rubber particles produces less transfer film, which leads to poor self-lubrication and severe friction coefficient fluctuations. With the increase of the volume fraction of micron rubber particles, the friction coefficient of the epoxy microcomposite surface increases due to the high toughness of the rubber particles.

Figure 44 (B) shows the changing curve of the friction coefficient of four epoxy microcomposites reinforced with the different concentration of micro-rubber particles at 40N load. Through observation, it can be found that the friction coefficient on the surface of epoxy microcomposite increases with the increase of particle concentration at 40N load, thus the particle concentration is in direct proportion to the friction coefficient of the material. The surface friction coefficient of neat epoxy and epoxy micro-composites with only 5% particle concentration tends to be stable. Compared with the 30N normal load, with the increase of the load, the wear of epoxy microcomposite and pure epoxy surface increases, which improves the self-lubrication effect. Furthermore, for epoxy microcomposites and pure epoxy materials with low concentration of rubber particles, the normal load only causes slight wear on the material surface and no fracture damage, so the friction coefficient is relatively stable. However, the surface cracks of epoxy microcomposites containing 12.5% and 15% rubber particle concentrations resulted in high friction coefficients.

4.3.2.1 Wear mass loss

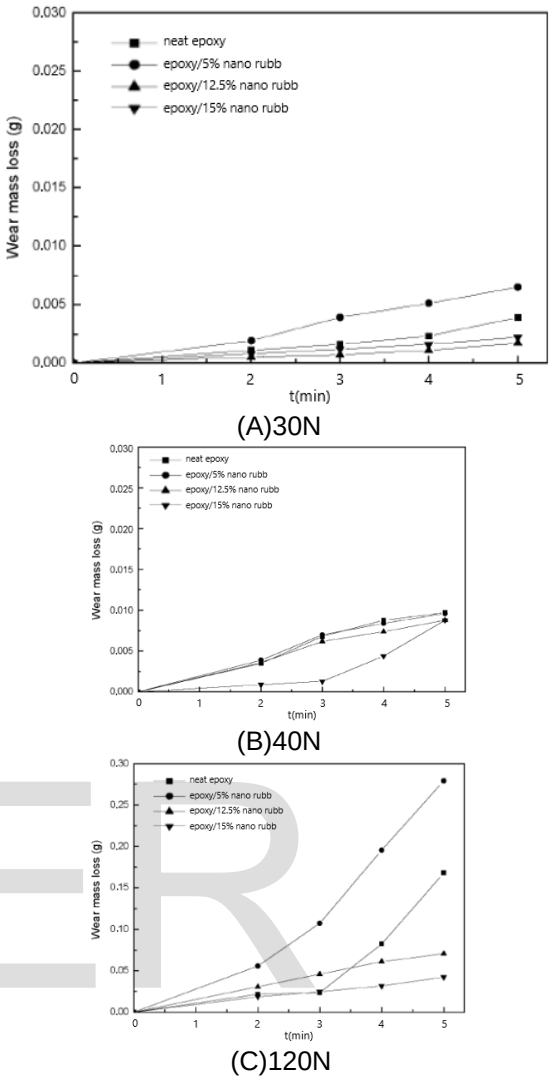

Figure 45 Effect of micro rubber concentration on wear mass loss of epoxy microcomposites (A-C).

Firstly, Figure 45 (A) describes the wear mass loss curves of four epoxy microcomposites with different concentrations of micro rubber particles at normal load of 30N. By analyzing these curves, it can be found that the wear mass loss of epoxy microcomposites reinforced by rubber particles of different concentration is low at 30N load, because the surface of epoxy microcomposites is only slightly worn at low load. Except for the neat epoxy, the wear mass losses of the other three kinds of reinforced epoxy microcomposites with different filling concentration particles increased linearly and the wear mass loss curves were relatively smooth. Among them, the epoxy microcomposite with 5% concentration of rubber particles had the greatest wear mass loss and the epoxy microcomposite containing 12.5% concentration of rubber particles had the least wear mass loss. The wear mass loss of pure epoxy is less than that of epoxy microcomposites containing 5% concentration of rubber particles but greater than that of epoxy microcomposites containing 15% concentration of rubber particles. Therefore, at 30N, the epoxy microcomposite containing 12.5% concentration of rubber particles has the best scratch resistance

and abrasion resistance.

Secondly, Figure 45 (B) shows the wear mass loss curve of epoxy microcomposites with different rubber particle concentrations at 40N load. By observing the figure, it can be seen that the trend of wear mass loss curve of epoxy microcomposites containing 15% concentration of rubber particles is different from that of epoxy microcomposites containing other three concentrations of rubber particles. Also, at the beginning of the test, the wear mass loss of epoxy microcomposite containing 15% volume fraction of rubber particles was the lowest, but its wear mass loss increased rapidly with the increase of the test time. The wear mass loss of neat epoxy and epoxy microcomposites containing 5% and 12.5% volume fractions of rubber particles increased in an equal proportional linear way at the beginning, but the growth rate of wear mass loss slowed down after the test time was 3 minutes. Furthermore, before the end of the wear test, the wear mass loss of the epoxy microcomposites reinforced with four kinds of rubber particles concentrations tended to be the same. The wear mass loss of neat epoxy and epoxy microcomposites with 5% rubber particle concentration at 40N load was greater than that of epoxy microcomposites with 12.5% and 15% rubber particle concentrations. Therefore, the surface of epoxy microcomposites reinforced with different concentrations of rubber particles had different damage mechanisms.

Moreover, the wear mechanism of materials surfaces can be further understood by comparing the friction coefficient curve with the wear mass loss curve. In Figure 45 (B), at 40N normal loading, the friction coefficients of the reinforced epoxy microcomposites containing 12.5% and 15% volume fractions of rubber particles were the same at 3 minutes 25 seconds of the simulation test, and the friction coefficient of the epoxy microcomposite with 15% volume fraction of rubber particles was lower than that of the epoxy microcomposite with 12.5% concentration of rubber particles. However, as shown in Figure 45 (B), when the simulation test was carried out at 3 minutes 25 seconds, the wear mass loss of epoxy microcomposites reinforced with 15% concentration of rubber particles was much lower than that of epoxy microcomposite reinforced with 12.5% concentration of rubber particles. As the simulation test continued from 3 minutes 25 seconds, the friction coefficient of the epoxy microcomposite reinforced by the rubber particles with a concentration of 15% continued to increase, but the friction coefficient of the epoxy microcomposite reinforced by the rubber particles with a concentration of 12.5% tended to be constant. Also, the wear mass loss of epoxy microcomposite reinforced by 15% concentration of rubber particles increased significantly, but the wear loss of epoxy microcomposite reinforced with 12.5% volume fraction of rubber particles slows down. The reason for this phenomenon is the effect of different concentration of rubber particles on wear properties of epoxy microcomposites.

Finally, by analyzing the wear mass loss curves of epoxy microcomposite reinforced by different concentrations of rubber particles in Figure 45 (C) at 120N high load, it can be found that, compared with the results in Figure 45 (A) and (B), the trend of wear mass loss curves of epoxy microcomposite reinforced by different concentrations of rubber particles is relatively changed. The wear quality of epoxy microcomposite containing 5% concentration of rubber particles and pure epoxy material at 120N normal load is different from that at low normal load. Also, by comparing the above three figures, it can be found that the wear mass loss of pure epoxy material and epoxy microcomposite reinforced with 5% volume fraction of rubber particles increases sharply and its growth rate increases gradually. For epoxy microcomposites reinforced with 12.5% and 15% volume fractions of rubber particles, there was no significant difference in wear loss at 30N, 40N and 120N normal loads, and the wear curves showed a linear growth trend. Furthermore, the surface of the neat epoxy material and the epoxy microcomposite reinforced with 5% concentration of rubber particles suffered severe wear at 120N normal load. As the applied normal load increases from 30N to 120N, the surface wear mechanism of the material changes from adhesive wear to fatigue wear, thus the variation of load has a great influence on the wear performance of epoxy microcomposite reinforced by low concentration of rubber particles and neat epoxy. However, with the increase of rubber particle concentration from 0% to 15%, the wear mass loss of epoxy microcomposite gradually decreased which illustrates that filling more rubber particles can effectively improve the toughness, scratch resistance and wear resistance of epoxy microcomposite.

CHAPTER V:CONCLUSIONS AND RECOMMENDATIONS

The main achievement of this project is to develop several new models for an in-depth understanding of the damage mechanisms of single-phase and multi-phase polymers. The research findings of this project are instructive for future research and development and applications in the field of material. Future scholars will be able to use the finite element models designed in this project to improve or study other polymer materials such as polyphenylene sulfite and poly-ether-ether-ketone. In this paper, the indentation and scratch performance of single-phase polymer pure epoxy and the scratch wear property of multi-phase polymer epoxy microcomposite were analyzed by finite element modeling method (FEM), the factors that may affect the mechanical properties of polymer materials were explored from shallow to deep. The fundamental conclusions obtained by analyzing the simulated results can be classified into the following points.

(1) During the indentation test of pure epoxy matrix, the von Mises stress of epoxy matrix increases with the increase of the indenter sharpness, and the von Mises stress of epoxy matrix is proportional to the indenter sharpness. Since the contact area between the sharp indenter and the epoxy matrix is the smallest, the plastic deformation of the epoxy matrix is the most obvious. Moreover, the maximum principal stress of the epoxy matrix is proportional to the indenter sharpness.

(2) For the scratch test of pure epoxy matrix, it shows that the maximum contact area between the spherical indenter and the material surface is the cause of the extremely uneven distribution of von Mises stress. The recovery of the scratch depth

which caused by spherical and blunt conical indenter indicates that single-phase polymers can be applied for the painting of products which at under low scratch conditions. Furthermore, extensive material removal caused by sharp conical indenter results in a transient concentration of compressive stress in tiny areas below the scratch tip and it causes the polymer surface to break.

(3) For the scratch test of multi-phase polymers, it can be known that the increase of particle concentration can make the stress distribution of the microcomposites more uniform and reduce the debonding phenomenon of the filling particles. The results also show that the residual scratch depth of soft particle modified polymer microcomposites is much higher than that of hard particle modified polymer microcomposites. Also, the change of hard particle size has no effect on the tensile stress of polymer materials. Furthermore, reducing the size of soft particles can delay the occurrence of cracking and the increase of the concentration of hard silicon particles can gradually change the surface cracking mode into the tensile mode, thus improving the scratch resistance of polymer microcomposites.

(4) For the wear test of epoxy microcomposites, the friction coefficient and wear mass loss of the single-phase polymer surface are proportional to the applied normal load, but the stability of the friction coefficient is inversely proportional to the load. The simulation results show that the wear mass loss increases rapidly at 120 N normal load. Also, filling low concentration rubber particles cannot improve the wear performance of multi-phase polymers and the enhancement effect is only achieved when the concentration of filling particle is equal to 12.5% or 15%. However, It was found that the polymer microcomposite modified with 12.5% concentration of rubber particles had the best wear performance, that is, the filling threshold of rubber particle concentration is close to 12.5%.

To sum up, the single-phase polymer cannot be used as the material for industrial products that may sustain trivial scratch damage such as automotive paint. The excellent scratch wear performance of multi-phase polymer enable it more wider applications rather than single-phase polymer in various industries. In addition, the simulation results show that the occurrence of microcracks in polyphase polymers is mainly determined by the maximum principal tensile stress, and the direction of the maximum principal stress determines the surface damage mechanism.The filling of soft particles makes the polymer matrix have higher toughness while the filling of hard particles makes the modulus and strength of polymer composites increase greatly.

ACKNOWLEDGMENT

The author wishes to grateful to the supervisor, Dr. Li Chang, for his efforts, patience and research ideas of finite element analysis. Also, the author heartfelt thanks to the Department of Mechanical Engineering of the University of Sydney for providing the necessary literature resources and suitable environment for the researches.

REFERENCES

[1] Atkins AG, Mai Y-W. Elastic and plastic fracture – metals, polymers, ceramics, composites, biological materials. Chichester: Ellis Horwood Ltd.; (1985).

[2] Kinloch AJ, Young RJ. Fracture behavior of polymers. New York: Elsevier Science Pub. Co.; (1983).

[3] ASTM International, ASTM G 171-03: Standard test method for scratch hardness of materials Using a Diamond Stylus, Annual Book of ASTM Standards, (2003),3:02.

[4] Hossain, M.M., Browning, R.L., Minkwitz, R., Sue, H.-J.: Efect of asymmetric constitutive behavior on scratch-induced deformation of polymers. Tribol. Lett. 47(1), 113–122 (2012).

[5] Hossain, M.M., Jiang, H., Sue, H.-J.: Efect of constitutive behavior on scratch visibility resistance of polymers—a finite element method parametric study. Wear 270(11–12), 751–759 (2011).

[6] Hossain, M.M., Jiang, H., Sue, H.-J.: Correlation between constitutive behavior and scratch visibility resistance of polymers— a fnite element method parametric study. In: SPE TPO Global Conference, Detroit, Michigan (2011).

[7] Nancy Staggers, Teresa Mccasky, Nancy Brazeltonect. Nanotechnology: The coming revolution and its implications for consumers, clinicians and informatics. Nurs Outlook. (2008), 56:268-274

[8] Li N., Huang Y, Du F.. Electromagnetic interference (EMI) shielding of single~walled carbon nanotube epoxy composites. Nano Letters, (2006), 6: 1141-1145.

[9] Edelstein A S, Cammarata R C. Nanomaterials: Synthesis, Properties and Applications. Bristol and Philadelphia: Institute of Physics Publishing. (1996), 5:13-19.

[10] Joseph Lik Hang Chau, Chun Ting Tung, Yu Ming Lin. Preparation and optical properties of titania/epoxy nanocomposite coatings. Materials Letters. (2008), 62: 3416-3418.

[11] Ke Yang Chuan, Wei Guang Yao, Wang Yi. Preparation, morphology and properties of nanocomposites of polyacrylamide copolymers with monodisperse silica. European Polymer Journal, (2008), 44:2448-2457.

[12] Hussain M.,Varley R.J., Mathys Z.. Effect of organo~phosphorus and nano-clay materials on the thermal and fire performance of epoxy resins. Journal of Applied Polymer Science. (2004), 91:1233-1253.

[13] Wetzel B, Haupert F, Zhang MQ. Epoxy nanocomposites with high mechanical and tribological performance. Composites Science and Technology. (2003), 63(14): 2055-2067.

[14] Zhang H, Zhang Z, Friedrich K, Eger C. Property improvements of in situ epoxy nanocomposites with reduced interparticle distance at high nanosilica content. Acta Materialia. (2006), 54(7):1833-1842.

[15] Wetzel B, Rosso P, Haupert F, Friedrich K. Epoxy nanocomposites-fracture and toughening mechanisms. Engineering Fracture Mechanics. (2006), 73(16): 2375-2398.

[16] Naous W, Yu XY, Zhang QX, Naito K, Kagawa Y. Morphology, tensile properties, and fracture toughness of epoxy/$A1_20_3$ nanocomposites. Journal of Polymer Science Part B-Polymer Physics. (2006), 44(10):1466-1473.

[17] Tjong SC. Structural and mechanical properties of polymer nanocomposites. Materials Science&Engineering R-Reports. (2006), 53(3-4):73-197.

[18] Qi Lai, Lee Burtrand I, Chen Sihai, Samuels William D, Exarhos Gregory J. High-dielectric-constant silver-epoxy composites as embedded dielectrics. Advanced Materials. (2005), 17(14): 1777-1781.

[19] Wang K, Chen L, Wu JS, Toh ML, He CB, Yee AF. Epoxy nanocomposites with highly exfoliated clay: Mechanical properties and fracture mechanisms. Macromolecules. (2005), 38(3): 788-800.

[20] Sun D, Chu CC, Sue HJ. Simple Approach for Preparation of Epoxy Hybrid Nanocomposites Based on Nanotubes and a Model Clay. Chemistry of Materials. (2010), 22(12): 3773-3778.

[21] Motta M, Li YL, Kinloch I, Windle A. Mechanical properties of continuously spun fibers of carbon nanotubes. Nano Letters. (2005) Aug, 5(8): 1529-1533.

[22] Song YS, Youn JR. Influence of dispersion states of carbon nanotubes on physical properties of epoxy nanocomposites. Carbon. (2005), 43(7): 1378-1385.

[23] Thostenson ET, Chou TW Processing-structure-multi-functional

property relationship in carbon nanotube/epoxy composites. Carbon. (2006), 44(14): 3022-3029.
[24] Ma HY, Wei GS, Liu YQ, Zhang XH, Gao JM, Huang F, et al. Effect of elastomeric nanoparticles on properties of phenolic resin. Polymer. (2005), 46(23): 10568-10573.
[25] Ma J, Mo MS, Du XS, Dai SR, Luck I. Study of epoxy toughened by in situ formed rubber nanoparticles. Journal of Applied Polymer Science. (2008), 110(1): 304-312.
[26] Le QH, Kuan HC, Dai JB, Zaman I, Luong L, Ma J. Structure-property relations of 55 nm particle-toughened epoxy. Polymer, (2010), 51: 4867-4879.
[27] S. Bahadur, A. Kapoor. The effect of ZnF_2, ZnS and PbS fillers on the tribological behavior of nylon 11.Wear, (1992), 155: 49-61.
[28] Q. Zhao, S. Bahadur. A study of the modification of the friction and wear behavior of polyphenylene sulfid by particle Ag_2S and PbTe fillers. Wear, (1998), 218: 62-72.
[29] Q. Zhao, S. Bahadur. The mechanism of filler action and the criterion of filler selection for reducing wear. Wear, (1999), 225-229: 660-668.
[30] Wand Qihua, Xu Jinfen, Shen Weichang, Liu Weimin. An investigation of the friction and wear properties of nanometer Si_3N_4, filled PEEK. Wear, (1996), 196: 82-85.
[31] Wand Qihua, Xue Qunji, Shen Weichang, Liu Weimin. The friction and wear properties of nanometer $Si0_2$ filled polyetheretherkutone. Trihology International, (1997), 30(3): 193-197.

[31] Wand Qihua, Xue Qunji, Shen Weichang, Zhang Junyan. The friction and wear properties of nanometer Zr02 filled polyetheretherketone. Journal of Applied Polymer Science, (1998), 69: 135-141.
[32] P. Sampathkumaran Kishore, S. Seetharamu, S. Vynatheya, A. Murali，R. K. Kumar. SEM observation of the effects of velocity and load on the sliding wear characteristics of glass fabric-epoxy composites with different fillers. Wear, (2000), 237: 20-27.
[33] Wang Hongtao, Liu Weimin, Yang Rongsheng, Xue Qunji. The friction and wear properties of nanometer $Si0_2$ filled polyetheretherkutone. Trihology International, (1997), 1(13): 79-82.
[34] S. Bahadur and D. Gong. The role of copper compounds as fillers in the transfer and wear behavior of PEEK. Wear, (1992), 154: 151-165.
[35] S. Bahadur and D. Gong. The role of copper compounds as fillers in the transfer film formation and wear of nylon, Wear, (1992), 154: 207-223.
[36] S. Bahadur, D. Tabor. The wear of filled polytetrafluoroethylene, Wear, (1984), 98:1-13.
[37] S. Bahadur and D. Gong. The friction and wear of nylon and CuS-nylon composites: filler proportion and counterface characteristics. Wear, (1993), 162-164: 397-406.
[39] F.P. Bowden and D. Tabor, The Friction and Lubrication of Solids, Oxford University Press, USA, (2001).
[40] C. Xiang, H.J. Sue, J. Chu, and B. Coleman, J. Polym. Sci., Part B: Polym. Phys., (2000), 39: 47 .
[41] P. Rangarajan, M. Sinha, V. Watkins, K. Harding, and J. Sparks, Polym. Eng. Sci., (2003), 43: 749 .
[42] ASTM D 7027–05. Standard Test Method for Evaluation of Scratch Resistance of Polymeric Coatings and Plastics Using an Instrumented Scratch Machine, ASTM International, (2005).
[43] Wang, Z., Gu, P., Zhang, H., Zhang, Z., Wu, X. Finite element modeling of the indentation and scratch response of epoxy/silica nanocomposites. Mech. Adv. Mater. Struct, (2014), 21: 802–809 .
[44] Moghbelli, E., Sun, L., Jiang, H., Boo, W.-J., Sue, H.-J. Scratch behavior of epoxy nanocomposites containing α-zirconium phosphate and core-shell rubber particles. Polym. Eng. Sci. (2009), 49: 483– 490 .
[45] Kurkcu, P., Andena, L., Pavan, A.: An experimental investigation of the scratch behaviour of polymers-2: infuence of hard or soft fillers. Wear, (2014), 317: 277–290.
[46] Hossain, M.M., Moghbelli, E., Jahnke, E., Boeckmann, P., Guriyanova, S., Sander, R., Minkwitz, R., Sue, H.-J. Rubber particle size and type efects on scratch behavior of styrenic-based copolymers. Polymer, (2015), 63: 71–81 .
[47] Ng, C.B., Schadler, L.S., Siegel, R.W. Synthesis and mechanical properties of TiO2-epoxy nanocomposites. Nanostruct. Mater, (1999), 12: 507–510 .
[48] Wang, Y., Lim, S.: Tribological behavior of nanostructured WC particles /polymer coatings. Wear, (2007), 262: 1097–1101.
[49] Naous W, Yu XY, Zhang QX, Naito K, Kagawa Y. Morphology, tensile properties, and fracture toughness of epoxy/Al_2O_3 nanocomposites. Journal of Polymer Science Part B-Polymer Physics. (2006), 44(10):1466-1473.
[50] Preghenella M, Pegoretti A, Migliaresi C. Thermo-mechanical characterization of fumed silica-epoxy nanocomposites. Polymer. (2005), 46(26): 12065-12072.
[51] Zunjarrao SC, Singh RP. Characterization of the fracture behavior of epoxy reinforced with nanometer and micrometer sized aluminum particles. Composites Science and Technology. (2006), 66(13): 2296-2305.
[52] Battistella M, Cascione M, Fiedler B, Wichmann MHG, Quaresimin M, Schulte K. Fracture behaviour of fumed silica/epoxy nanocomposites. Composites Part a-Applied Science and Manufacturing. (2008), 39(12): 1851 — 1858 .

[53] Zhao S, Schadler LS, Duncan R, Hillborg H, Auletta T. Mechanisms leading to improved mechanical performance in nanoscale alumina filled epoxy. Composites Science and Technology. (2008), 68(14):2965-2975.
[54] Zhang H, Zhang H, Tang LC, Liu G, Zhang DJ, Zhou LY, et al. The effects of alumina nanofillers on mechanical properties of high-performance epoxy resin. Journal of Nanoscience and Nanotechnology. (2010), 10(11):7526-7532.
[55] Ragosta G， M, Musto P, Scarinzi G, Mascia L. Epoxy-silica particulate nanocomposites: Chemical interactions, reinforcement and fracture toughness. Polymer. (2005), 46(23):10506-10516.
[56] Ma J, Mo MS, Du XS, Rosso P, Friedrich K, Kuan HC. Effect of inorganic nanoparticles on mechanical property, fracture toughness and toughening mechanism of two epoxy systems. Polymer. (2008), 49(16):3510-3523.
[57] Mahrholz T, Stangle J, Sinapius M. Quantitation of the reinforcement effect of silica nanoparticles in epoxy resins used in liquid composite moulding processes. Composites Part A: Applied Science and Manufacturing. (2009), 40(3): 235-243
[58] Huang CJ, Fu SY, Zhang YH, Lauke B, Li LF, Ye L. Cryogenic properties of SiO_2/epoxy nanocomposites. Cryogenics. (2005), 45(6):450-454
[59] Guo ZH, Pereira T, Choi O, Wang Y, Hahn HT. Surface functionalized alumina nanoparticle filled polymeric nanocomposites with enhanced mechanical properties. Journal of Materials Chemistry. (2006), 16(27):2800-2808.